TEM and EDS characterization in a Bennettitalean cuticle from the Lower Cretaceous Springhill Formation, Argentina

Gaëtan Guignard, Martín Carrizo, Maiten Lafuente Diaz, Georgina del Fueyo

TEM and EDS characterization in a Bennettitalean cuticle from the Lower Cretaceous Springhill Formation, Argentina

Gaëtan Guignard, Martín A. Carrizo, Maiten A. Lafuente Diaz, Georgina M. Del Fueyo

PII: S0034-6667(23)00174-4

DOI: https://doi.org/10.1016/j.revpalbo.2023.105005

Reference: PALBO 105005

To appear in: *Review of Palaeobotany and Palynology*

Please cite this article as: G. Guignard, M.A. Carrizo, M.A. Lafuente Diaz, et al., TEM and EDS characterization in a Bennettitalean cuticle from the Lower Cretaceous Springhill Formation, Argentina, *Review of Palaeobotany and Palynology* (2023), https://doi.org/10.1016/j.revpalbo.2023.105005

TEM and EDS characterization in a Bennettitalean cuticle from the Lower Cretaceous Springhill Formation, Argentina.

Gaëtan Guignard[a], Martín A. Carrizo[b], Maiten A. Lafuente Diaz[b], Georgina M. Del Fueyo[b]

[a]Université Lyon 1, CNRS, ENTPE, UMR 5023 LEHNA, 69622 Villeurbanne, France. gaetanguignard@orange.fr

[b]Museo Argentino de Ciencias Naturales "Bernardino Rivadavia", CONICET, Av. Ángel Gallardo 470, CP 1405, Buenos Aires, Argentina. blackdisk@gmail.com; maitenlafuentediaz@gmail.com; georgidf@yahoo.com.ar

Corresponding author:

Family name: Carrizo

First and second names: Martín Alejandro

Postal address: Av. Ángel Gallardo 470, (1405) Buenos Aires, Argentina.

Telephone number: + 54- 011-4982-6595

e-mail address: blackdisk@gmail.com

Running head: Guignard et al. – TEM and EDS studies of Bennettitalean fronds.

Abstract

New cuticle samples from the bennettitalean *Ptilophyllum eminelidarum* were herein studied using the combination of light microscopy (LM), scanning and transmission electron microscopy (SEM, TEM), and element analysis by Energy Dispersive Spectroscopy (EDS). The new TEM studies correspond with and improve

the former ones; however, statistical measurements reinforce their uniqueness and erect Bennettitales as a heterogeneous group of cuticles. Six types of cuticles were recognized. According to the factorial component analysis (FCA), the cuticles of the stomatal apparatus show the highest level of interest, while the epidermal cell cuticles, the lowest. For the 9 variables, the top 6 as to importance were the most independent, which could be used as criteria for identification in Bennettitales. A dichotomous key was built, allowing for a rapid identification of each of the 6 types of cuticles based on the 9 variables. Showcasing an upper cuticle significantly thicker and more exposed, and a thinner lower cuticle that is normally more protected, the micropalaeoenvironment of these leaves is of interest. The taxonomical identity of the present taxon is also revealed by the EDS values; S/Ca ratio is homogeneous for all layers of both cuticles, leading to assume, with extreme precaution, a putative similar influence of the palaeoenvironment on these two opposite surfaces of the leaf. As the first detailed statistical TEM and EDS for the Bennettitales, it highlights the great interest of this type of studies and the strong interest for revealing the characters of each type of cuticle and layer.

Keywords: TEM, EDS, Cuticle, Bennettitales, Lower Cretaceous, Patagonia, Argentina

1. Introduction

The role of cuticles in systematic and taxonomical studies has become widely recognized since the work of Brongniart in 1834. This author used the word “cuticule” (= cuticle) to refer to an extraction of the cuticle in living plants, which he then illustrated with hand-drawn figures (Brongniart, 1834: plates 2 and 3). The cuticle’s high resistance to decay makes it a valuable source of palaeobotanical information,

having contributed not only with palaeobiological and palaeoecological considerations, but also having proved to be crucial for species identification (Thomas, 1949; Florin, 1958; Harris, 1964; Oldham, 1976; Archangelsky and Taylor, 1986; Archangelsky et al., 1986; Cleal and Zodrow, 1989; Kerp, 1990; Carrizo et al., 2014, Guignard et al., 2016; Carrizo et al., 2019a; among others).

Nowadays, several insights into plant cuticles have become more frequent through research papers, updated reviews, and special issues (González-Valenzuela et al., 2023; Molina et al., 2023), e.g. in their biosynthesis (Liu et al., 2022; Wang and Chang, 2022) or formation (Berhin et al., 2022; Philippe et al., 2022). Especially regarding the details of cuticle structure, Raman imaging detailed its different parts (Bock et al., 2021) whereas the complex architecture was studied through chemical analyses (Reynoud et al., 2021, 2022). In living plants, few studies used transmission electron microscopy (TEM). Nevertheless, TEM was used quite recently in living Coniferales (*Pinus uncinata* Ram.) (Rueno et al., 2022), and in several angiosperms such as for trichomes of *Metrodorea nigra* A. St.-Hil. Rutaceae (Machado et al., 2023); for leaves domatia of the three Rubiaceae *Gardenia thunbergia* Thunb., *Rothmannia capensis* Thunb., and *Rothmannia globosa* (Hochst.) Keay (Situngu and Barker, 2022); or for the adhesive secretion in *Schizolobium parahyba* (Vell.) Blake Leguminosae, Caesalpinioideae (Paiva et al., 2022).

The remains of plants' cuticles, along with woods and spores-pollen, are the most available in the fossil record (Guignard et al., 2021). The cuticles are of great interest, especially given that TEM provides very fruitful data concerning to taxonomy and palaeoenvironment (Guignard, 2019). As it was revealed by Carrizo et al. (2019a), the cuticular studies are of great importance in groups where the leaves are quite similar

among species and, therefore, difficult to differentiate using only their general morphological aspect, as is the case of the Bennettitales.

Characterized by its leaflets attached to the upper surface of the rachis and their asymmetrical base composed of a decurrent lower margin, *Ptilophyllum* Morris is one of the most common bennettitalean leaves found in the Lower Cretaceous Springhill Formation in the province of Santa Cruz, Argentina, with numerous species already described (Archangelsky, 1976; Archangelsky and Baldoni, 1972; Baldoni, 1979; Baldoni and Taylor, 1983; Carrizo and Del Fueyo, 2015; Carrizo et al., 2019a; Lafuente Diaz et al., 2019).

Taking the opportunity of the recent erection of *Ptilophyllum eminelidarum* Carrizo, Lafuente Diaz et Del Fueyo 2019 with a first brief TEM results, the objective of this contribution is to conduct further investigations on the leaves of this bennettitalean fossil species based on statistical details of cuticle ultrastructure using TEM and element analysis by Energy Dispersive Spectroscopy (EDS). Our purpose is to fully characterize this taxon, to compare it with other bennettitalean species, and to reveal some taxonomical and palaeoenvironment aspects.

Finally, this article is included in a special issue dedicated to Sergio Archangelsky, following his famous remark -with collaborators- pronounced in one of his pioneering first papers on fossil cuticles in 1986 against critics, about "…the assumption that cuticle fine structure could offer no additional information that could not be determined with either transmitted light or scanning electron microscopy." This article is, once more, proof of the great potential that these research topics still hold for improving our understanding of fossil cuticles.

2. Geological and palaeobotanical background

The Springhill Formation (Thomas, 1949) occurs in the NNW sector of the Austral Basin, covering the south of Argentina and Chile. Due to the transgressive characteristics of its deposits and its significant areal distribution, the age of this formation varies from location to location, being late early Hauterivian/early Barremian at the proximities of the Estancia El Salitral locality, and Valanginian/Hauterivian and Berriasian?/Valanginian-early Hauterivian at the subsurface of Chile, Tierra del Fuego province, and the Continental Platform of Argentina (Riccardi, 1976; Cortiñas and Artabe, 1981; Ottone and Aguirre-Urreta, 2000; Giacosa and Franchi, 2001; Archangelsky and Archangelsky, 2004; Spalleti et al., 2009).

The palaeobotanical composition of the Springhill Formation includes representatives of five important divisions (Pteridophyta, Pteridospermophyta, Cycadophyta, Gingkgophyta, and Pinophyta) of which the Cycadophyta is dominant, with more than 50% of the total diversity. Within this latter group, the Order Bennettitales is the most abundant, far over the Cycadales, with a record that includes several bracts of *Cycadolepis* Saporta and leaves of *Otozamites* Braun and *Ptilophyllum* Morris (Carrizo and Del Fueyo, 2015).

The genus *Ptilophyllum* has a strong dominance in the fossil record of the Springhill Formation, its leaves being one of the most common fossils, with variable sizes and morphologies. Some of its representatives are *P. ghiense* Baldoni from the Río Correntoso locality; *P. valvatum* Villar de Seoane and *P. angustus* Baldoni et Taylor from the Estancia El Salitral locality; and *P. antarcticum* Archangelsky et Baldoni from core samples of Argentina and Chile (Archangelsky, 1976; Archangelsky and Baldoni, 1972; Baldoni, 1979; Baldoni and Taylor, 1983).

In recent years, numerous prospections have been carried out at the proximities of the Estancia El Salitral and to the north of the Ghío Lake, in the Santa Cruz province of Argentina (Plate I, 1), substantially increasing the number of species studied and the diversity composition of the megaflora of the Springhill Formation (Carrizo and Del Fueyo, 2015). These studies comprised the erection of two Bennettitalean species: *Ptilophyllum micropapillosum* (Lafuente Diaz et al., 2019) and *P. eminelidarum* (Carrizo et al., 2019a). The latter is the objective of this contribution.

3. Material and methods

The fossils were recovered from pelitic levels of the Springhill Formation that outcrops at the Río Correntoso locality, Santa Cruz province, Argentina (Plate I, 1). The specimens studied herein comprise new cuticle extractions from leaves of *Ptilophyllum eminelidarum* Carrizo, Lafuente Diaz et Del Fueyo (MPM-PB 15347-15348).

For the extraction and processing of the cuticles, the same methodology detailed in Carrizo et al. (2019a) was followed. The cuticles are very well preserved. Some of them were gently removed from the sediment, oxidized in 40% nitric acid followed by 5% ammonium hydroxide, stained with safranin and mounted in glycerin jelly to be observed with LM. For SEM observation, the cleaned cuticles were mounted on exposed film, glued to stubs, and coated with gold-palladium. LM observations were made with a Leica DM 2500 microscope and the micrographs were taken with a Leica DFC 280 and a Leica ICC50 cameras. SEM observations were made under a Philips XL30 TMP SEM at 15.1 kV equipment at the Museo Argentino de Ciencias Naturales “Bernardino Rivadavia”.

For TEM, pieces of cuticles were prepared using an efficient technique (Lugardon, 1971), as described in detail with photos (Guignard, 2021), also used for living plant

cuticles (Bartiromo et al., 2012, 2013). In total, 3 untreated pieces of leaflet cuticles from the same frond were embedded in Epon resin. From those, 100 ultrathin 60-70 nm sections were collected on uncoated and Formvar (half and half) 200 Mesh hexagonal copper grids. Ultrathin sections were stained with uranyl acetate (15 nm) and lead citrate (20 mn.), and selected, observed, and photographed with a Philips CM 120 at 80 kV equipment, at the Centre de Technologie des Microstructures (CTμ) of Lyon-1 University, France.

Sections of 1 μm for LM were performed, and then stained following the classical method (Richardson et al., 1960) with methylene blue and Azur II solution (½-½), at the Centre de Technologie des Microstructures (CTμ) of Lyon-1 University France. The equipment used was a Zeiss Axioskop 2 Optical Microscope with a Zeiss Axiocam ERC 5s Camera. The image acquisition software was ZEN.

For EDS, 5 osmium (Os) pre-stained ultrathin 60-70 nm sections devoid of uranyl acetate and lead citrate staining were cut. An EDS analysis was performed on the TEM using three unstained grids. The microscope was a TEM JEOL 2100F, operated at 200 kV in STEM-HAADF imaging mode (spot size 1 nm), and coupled with EDS analysis. The spectrometer was an Oxford X-Max 80 mm² and the analysis software was AZTEC. Among the elements detected, Cu and Al were eliminated in the results as they belonged to the grids, Os was eliminated as part of the embedding technique, Si was eliminated as part of the oils used in the TEM, as well as C and O, also eliminated as major parts of the EPON embedding resin.

Measurements were evaluated with the Student's t-test and the Mann-Withney test, and multidimensional analyses (factorial and hierarchical component analyses FCA and HCA) were all performed using XLSTAT software version 2023, statistical and

analysis solution, Paris France, https://www.xlstatt.com. All diagrams included in this paper were provided by the same software.

The terminology used for TEM follows the international description of cuticles and their layers (Archangelsky and Taylor, 1986; Holloway, 1982), updated in Figure 1 of a recent review (Guignard, 2019), and takes into account new precise TEM observations on various fossil taxa.

All the materials of *Ptilophyllum eminelidarum* are deposited in the Paleobotany Collection of the Regional Museum Padre MJ Molina, Río Gallegos, Santa Cruz Province, under the acronym MPM-PB.

4. Results

4.1 Brief description of leaf morphology

The specimens of *Ptilophyllum eminelidarum* consist of compressions of pinnate leaves up to 15 cm long and 7 cm wide (Plate I, 2) with leaflets alternate to sub-opposite arranged, in angles that vary from 45º to 80º in the proximal part of the leaf, decreasing distally. The size of the leaflets varies along the leaf, from 4 cm long and 0.44 cm wide (the largest) at the base, to 3 cm long and 0.25 cm wide (the smallest) at the apex. Most of the leaflets are linear with the distal portion slightly falcate. They have an entire upper margin and a decurrent lower margin, as is common for the genus.

The diagnostic characteristics of this species lie on its cuticular features. With hypostomatic leaves, the lower epidermis bears two distinct, uniformly distributed papillae morphologies: the compound papillae (30-50 µm wide), on the epidermal cell above the veins, and the small simple papillae (12-15 µm wide) on the epidermal cells between the veins (Plate I, 3-5 and II, 1-4). The compound papillae have an oval-

rectangular base cell, and each papilla shows 5 to 10 irregular lobulated segments that, in some cases, can be fused with other segments of neighboring papillae (Plate I, 5 and II, 4). The simple papillae are mostly dome-shaped and are always located near the stomatal rows (Plate I, 3,4 and II, 1,3). The stomata are distributed between the veins in 2 or 3 rows of a mean of ~168 µm wide. They are mostly aligned, perpendicularly oriented to the venation. The stomatal apparatus is paracytic, subrectangular, 30-45 µm wide and 40-60 µm long, with two isodiametric subsidiary cells, and sunken guard cells (Plate I, 3 and II, 6).

Conversely to the lower epidermis, the upper cuticle is smooth and consists of quadrangular to polygonal ordinary cells of varying sizes, with markedly sinuous anticlinal walls (Plate I, 6 and II, 5).

4.2 TEM results

Due to the high number of grids observed, all cuticles were characterized by a complex combination of layers observed in majority of cases, which represent their identities, allied with other combinations observed in minority, showing the complexity of this taxon.

The cuticular membranes CM of both upper (1.95 µm in mean, minimum 0.71 and maximum 2.73; table 1) and lower (1.43 µm in mean, 0.71-2.47) epidermis are largely made with an A2 granular layer of the cuticle proper (14.72 and 14.42% of the total CM, respectively), a B1 fibrillar layer (68.87 and 61.53% of the total CM, respectively) with fibrils oriented mostly parallelly to the surface of the cuticle, and a B2 granular layer (16.41 and 24.05% of the total CM, respectively) of the cuticular layer (Plate III 1,2, Plate V 1-5).

Other combinations occur in a minority of cases, as the upper cuticle may also have only B1 and B2 layers (Plate III 3-5), or A2 and B1 layers (Plate III 6-8); while the lower cuticle may have B1 and B2 layers (Plate V 6,7), only B1 (Plate V 8,9), or only A2 (Plate V 10,11) layers.

The edges of leaves (Plate IV 1-13) show the connection between upper and lower cuticles, with A2 and B1 layers fairly heterogeneous in their distribution, probably related to the very curved cuticles in these areas. B1 fibrils may even be oriented quite at random (Plate IV 8,9).

In their majority, the cuticles of simple (1.23 µm in mean, 1.15-1.40; table 1, Plate VI) and compound (5.34 µm in mean, 4.06-6.50; Plate VII) papillae of the lower cuticle are made with an A2 granular layer of the cuticle proper (8.96 and 19.86% of the total CM, respectively), a B1 fibrillar layer of the cuticular layer (91.04 and 80.14% of the total CM, respectively) with fibrils oriented mostly parallelly to the surface of the cuticle. However, in the edges (Plate VI, 6) B1 fibrils may even be oriented quite at random. As shown in these photos (especially plate VII), the concentration of fibrils may be quite low and faintly contrasted, especially in the middle parts of the cuticles.

Other combinations occur in a minority of cases, as simple papillae cuticles may have an added B2 layer (Plate VI, 9,10), while compound papillae cuticles may present only a B1 layer (Plate VII, 10-12) with very low concentration of fibrils in the upper part, only faintly stained but much more visible using artificial coloration, increasing the contrast of the fibrils compared with the black and white colours.

In their majority, the cuticles of stomatal apparatuses are made with a B1 fibrillar layer of the cuticular layer, oriented mostly parallelly to the surface of the cuticle (table 1, Plates VIII and IX). The subsidiary cell cuticle (2.10 µm in mean, 0.11-

9.86) shows various concentrations of fibrils. The guard cell cuticle was 0.34 µm in mean (0.09-1.19) and looks more homogeneous in the number of fibrils.

In a minority of cases, as in ordinary epidermal cell cuticles, the three A2, B1, and B2 layers occur for the two types of cell cuticles (Plate VIII 5,6, Plate IX 5), which correspond to an increasing number of granules making an outer A2 and an inner B2 layers, with an absence of fibrils in these zones.

4.3 EDS results

Among the elements analyzed (Appendix A) in the upper and lower ordinary epidermal cell cuticles sections embedded in resin, a comparison-check of "only" resin part of the section, beside the cuticle section, was realized. Chlorine (Cl) appears in both resin and cuticles, CL and calcium (Ca) plus sulfur (S) in the cuticles. As the data of the cuticle elements obtained (mixed with resin due to the technical procedure) may include those from the embedding resin, the value of Cl from the resin alone should be lower than cuticle + resin values. Cl was homogeneous in lower and B2 layers (= unsignificant differences, Fig. 1-A), while it was significantly different from the other four layers (A2 and B1 of both upper and lower layers, p values between 0.012 and 0.021). However, as these four latter potentially significant values of cuticles they were lower than "only" resin value, none of these Cl values can be considered for the comparisons, just Ca and S were taken into account for the cuticles.

As the absolute values of the elements analyzed by each spot were not entirely comparable, only ratios between elements were taken into account. Therefore, only the S/Ca ratio is considered for the cuticles (Fig. 1-B). As Mann-Whitney test shows only insignificant differences between the ratios of each of the six layers, this ratio proves

homogeneous and has a mean of 0-0.56 (minimum of 0 and maximum of 0.62), summarizing all layers of the two types of upper and lower cuticles.

5. Discussion

5.1 LM and SEM observations

The LM and SEM observations of the new cuticle samples show all the characteristics expected for *Ptilophyllum eminelidarum*. All the new measurements, from the size of the leaves and leaflets to the size of cells and papillae, as well as the form, distribution, and number of lobules of the papillae, are in concordance with the previous study of this species (Carrizo et al., 2019a).

5.2 TEM considerations

Although cuticles were defined by their layers after taking 30 measurements for each of them, in the study herein we analyze separately cuticles and layers considerations, and then make a synthesis between them. All measurements concern the cuticle details observed in the majority of cases provide the most accurate synthesis. These considerations include the 6 types of cuticles (namely upper and lower ordinary epidermal cell cuticles U-OEC and L-OEC, subsidiary and guard cell cuticles of the stomatal apparatus SC and GC, and simple and compound papillae cuticles simp-pp and comp-pp), along with the 9 variables of the layers' thickness values and thickness percentages (namely A2 mean and A2%, B1 mean and B1%, and B2 mean and B2%), comprising the total layers = cuticular membrane CM mean (composed of cuticle proper

CP = A2 layer mean and %, and cuticular layer CL mean and % = B1 + B2, all possibilities depending on the types of cuticles).

5.2.1 Types of cuticles

The result of the factorial component analysis (FCA) with chi-square of the 6 types of cuticles (Appendix B) has an observed value of 2266.7, largely higher than the critical value (55.8), demonstrating a very significant link between cuticles and layers. The outstanding quality of the analysis was also supported by 99.4% of the information on the three first axes retained in the study. Axis 1 has almost 2/3 of the information (64.73%) while axis 2 has about 1/4 (25.75%); axis 3 contains some residual but interesting information separating some cuticles, with a little bit less than 1/10 of information (8.94%). The three-dimensional representation of the 6 types of cuticles (Fig. 2, Appendix C) brings new information, compared with the former study of this species (Carrizo et al., 2019a), where ordinary epidermal cell and papillae cuticles were described. In the present study, the utmost importance of the stomatal apparatus cuticles compared with ordinary epidermal cell and papillae cuticles is revealed. This FCA provides the following hierarchy with two sets of cuticles: firstly, subsidiary and guard cells, and a lower ordinary epidermal cell with a cumulative contribution to the three axes of 0.44-0.48 (SC and GC being at the first and second rank); then, an upper ordinary epidermal cell, and compound and simple papillae with 0.20-0.32 (papillae cuticles being at the two last ranks). The order of importance of the cuticle types is as follows: SC GC (of the stomatal apparatus), L-OEC, U-OEC (both epidermal cell cuticles), comp-pp and simp-pp (both papillae cuticles). FCA shows that ordinary epidermal cell cuticles are intermediate in their contribution to the axes, and that both types of papillae contribute the least to the axes.

The Student's t-tests (Fig. 4, Appendices D,E) allow us to present, for the first time in TEM cuticle studies, a synthesis for each type of cuticle, taking into account both thickness values and percentages of each layer. Each type of cuticle is represented by the mean of all of its layers (Figs. 5,6). For each cuticle, each layer has the ratio of the total significant differences between said cuticle and all the other same layers of the other cuticles/all possible combinations (significantly or not significantly different) for each layer. The most significant differences presume a higher independence of each cuticle compared with all others, whereas the less significant differences represent a lower independence of each cuticle. Firstly, the summarized figures reveal, for all cuticles, high independence compared between one another. Their independence level for thickness values was 60-87%, while for thicknesses percentages it was higher, about 57.5-100%. Although it is the first time that this independence is highlighted thanks to Student's t-tests, these first statistical details in Bennettitales seem to show quite a higher individuality of the cuticles than the other taxa already studied through statistics (Guignard, 2019). Secondly, the comparison between the two sets of cuticles of FCA indicates the following results. It is worth noting that the 3 most important cuticles (SC, GC, L-OEC) are the least independent (a mean 75.7% of independence), i.e., they are the most dependent among themselves. This seems rather congruent, as they all belong to the lower cuticle. Conversely, the 3 less important cuticles (U-OEC, comp-pp, simp-pp) are the most independent (a mean 86%), i.e., they are the least dependent among themselves, which is also congruent, as they belong to both upper and lower cuticles. This could lead to the idea of the individualization of each upper and lower cuticle, roughly variable in other taxa (Guignard, 2019).

5.2.2. Layers' details

As a result of the 30 measurements obtained for each layer, and the thickness means and percentages calculated (table 1), a three-dimensional reconstruction was provided (Fig. 7). The reconstruction includes details of the 6 types of cuticles and their A2 (or lack of A2), B1 and B2 (or lack of B1 and B2) layers. The upper and lower ordinary epidermal cell cuticles comprised A2, B1 and B2 layers. Such a cuticle formula, as previously defined (Guignard, 2019), corresponds with the former study of this taxon (Carrizo et al., 2019a). Moreover, the TEM thicknesses provided are included within the range of the present study, except the maximum values of CM and B1. As in the former TEM observation, no A1 layer was observed in the present study; although in many cases the outermost part of the cuticle was not very straight, which could be explained by some degree of damage on the cuticle. In the (minor) cases where it was straight, the A1 layer was absent. This cuticle formula for U-OEC and L-OEC (A2-B1-B2) corresponds to none of the other taxa, fossil families or orders already studied in detail, such as, in Coniferales: Araucariaceae (Carrizo et al., 2019b), Cheirolepidiaceae (Guignard et al., 1998; Yang et al., 2009; Guignard et al., 2017; Yang et al., 2018), Miroviaceae (Nosova et al., 2016), and in living Pinaceae (Bartiromo et al., 2012); in the Ginkgoales *Baiera-Sphenobaiera* cuticle group (Guignard et al., 2019; Wang et al., 2005), and the *Ginkgo-Ginkgoites-Pseudotorellia* group (Guignard and Zhou, 2005; Del Fueyo et al., 2006; Del Fueyo et al., 2013; Guignard et al., 2016; Nosova et al., 2019); in Pteridospermales [(Guignard et al., 2001; Thevenard et al., 2005); Corystospermaceae (Guignard et al., 2004; Martinez et al., 2020)] and cycadalean cuticles (Artabe et al., 1991; Archangelsky et al., 1995; Passalia et al., 2010). The only taxa with the abovementioned three layers showed different taxonomical affinities: one species of Caytoniales (Carrizo et al., 2014), and two of Czekanowskiales (Zhou and

Guignard, 1998), but that was only true for their upper cuticle, their lower cuticles being different.

Inasmuch as this is the first detailed statistical analysis made in *Ptilophyllum eminelidarum* cuticles, it will be used as the basis for further studies in Bennettitales. Specifically, studies might deal with a so-called homogeneous (order or family) group (Guignard, 2019) with only one cuticle formula, or with a heterogeneous group with various types of cuticles in one family or order (5 and 3, respectively).

Unfortunately, other taxa of Bennettitales already studied with TEM failed to provide enough statistical measurements (Villar de Seoane, 1995, 1999, 2001). These taxa are *Ptilophyllum longipinnatum* Menéndez, *P. hislopi* (Oldham) Seward (Menéndez, 1966; Villar de Seoane, 2003), and *P. antarcticum* (Barale and Baldoni, 1993), which show heterogeneity in the photos and descriptions, and therefore, the second hypothesis would seem more conceivable. This is also at least congruent with the remarks that, in Bennettitales, "… the complexities of the group are now only becoming apparent." (Taylor et al., 2009).

A significant issue concerns the guard cell cuticle, which is of interest among various taxa, as it is fairly often different from the ordinary epidermal cell and subsidiary cell cuticles, but which allows for a quite precise identification of orders (Guignard, 2019). In the present study, the guard cell cuticle, just made with a B1 layer, is also different from OEC cuticles. These cuticles are included within the Coniferales group (Guignard, 2019; fig. 4), with *Brachyphyllum garciarum* Carrizo, Del Fueyo, Lafuente Diaz et Guignard of the Araucariaceae (Carrizo et al., 2019b). They also have a single B1 layer, however the measurements are different, and the two cuticles show their own identities: thickness of a mean 1.34 µm (0.70–1.94) versus a mean 0.34 µm (0.09-1.19) in the present *Ptilophyllum* study (table 1).

The FCA (Fig. 3, Appendix D) provides the following hierarchy with three sets of variables: B2 and A2 means contribute the most to the axes (0.416-0.549); followed by B1 %, CL % and B1 mean (0.264-0.326); and finally, B2 %, A2 %, CL mean and CM mean (0.075-0.145). From this arrangement, it is clear that the thinner granular layers (B2 and A2) are the most important, while the B1 thicker fibrillar layer is not so important- in fact, the least important variable is the total thickness of the cuticular membrane CM. This last point is congruent with the FCA developed for these 41 cuticles and 23 variables (Guignard, 2019) with diverse taxa (except Bennettitales), enhancing the great interest of detailed TEM studies and the potential interest of each layer, instead of just providing the total thickness of the cuticular membrane. However, some new elements seem to arise in Bennettitales with other combination(s) of variables, demonstrating their potential individuality. The B1 fibrillar layer is not so important in the present study (it was quite important in the other FCA without Bennettitales), even though A2 was present in the first set of variables in the two FCA. Finally, in the present FCA, the thickness percentage values are overall less contributing to the axes than the thickness. The case was very different for the former FCA (Guignard, 2019) where B2% and B1% were in the first set of variables.

The Student's t tests also allowed us to present, for the first time in TEM cuticle studies, a synthesis for each of the 9 variables (Fig. 4, Appendices D,E). Firstly, the summarized figures (Figs. 5,6) reveal, for all variables, an independence that proves different than the independence for types of cuticles; it is less variable for their thickness values (73-87 %), while for their thickness percentages it is 0-87%. If a comparison is made with other taxa already studied through statistics, despite this being the first time that independence was enhanced thanks to Student's t-tests, all parts seem to be in the same range (Guignard, 2019). Secondly, if a comparison is drawn among

the three sets of variables of FCA, it must be noted that the 6 most important variables (B2 and A2 means, B1 and CL %, B1 mean) are, conversely to the most important cuticles, the most independent (a mean of 83.5%). For example, the less dependent among them demonstrate their higher contribution to the FCA axes; conversely, the 4 less important cuticle variables (B2 and A2 %, CL and CM means) are the less independent (a mean of 57.25%). Also, the most dependent among them explain their smaller contribution to the FCA axes. This could lead to the idea of giving a preference to the first variables for identification in Bennettitales, as already discussed by Guignard (2019).

5.2.3 Synthesis between variables and layers

The complementarity among the 9 variables, their hierarchy established by FCA with chi-square, their independence found with Student's t-tests, together with a hierarchical component analysis (FCA) with chi-square, enable us to build a dichotomous key (Fig. 8), in which the identification of each of the 6 types of cuticles is based on very few variables. Two groups of cuticles (OEC cuticles, or stomatal apparatus and papillae cuticles) are separated selecting, at first, only the presence or absence of the B2 layer (the most important in FCA). Secondly, two sub-groups are distinguished (stomatal apparatus or papillae cuticles, all from the lower cuticle) taking into account only the presence or absence of an A2 layer. Finally, within each of these three entities (OEC, stomatal apparatus, and papillae cuticles) with the remaining variables (thickness values and percentages, intermediate in importance through FCA, or the least important), each group is divided in two and each type of cuticle is identified. The HCA drawn in the lower part of the key reinforces these identifications, with some differences in the variables. The presence or absence of B2 separates the two

groups at the scale 1; then, GC is separated at the scale 0.7 (because of small values of mean B1 = CL = CM, as GC is only made with a B1 layer). Subsequently one papilla was separated at the scale of 0.6, finally SC and the other papilla were separated at the scale of 0.2. In the FCA tree we can just notice some overlap between SC and papillae, which is not the case for the above-described hierarchy. In this key, the two OEC are the less independent (= the most dependent), whereas the most independent are the two papillae cuticles (= the less dependent). This independence-dependence may also be used as a criterion to identify each of the three entities (OEC, stomatal apparatus, and papillae cuticles).

5.3 TEM and the palaeoenvironment

In a TEM study on the cuticle ultrastructure of a fossil bennettitalean (Barale and Baldoni, 1993) a possible relation between cuticle details and the palaeoenvironment was reported; however, it was linked with a zone between the polylamellate layer of the cuticle and the outermost wax. Some years later, Villar de Seoane (2001) noted that the TEM cuticle details of some Bennettitales could be related to the palaeoenvironment (volcanic activity). Nonetheless, since then, the lack of detailed TEM comparisons between taxa and localities for Bennettitales renders the palaeoenvironmental relationship with the details of the layers still poorly documented.

More recently, Guignard (2019) defined two kinds of palaeoenvironments for the cuticles: macro and micropalaeoenvironments. The macropalaeoenvironment refers to the "palaeoenvironments of the localities sensu lato". According to Carrizo et al (2019a), *Ptilophyllum eminelidarum* was living in "…a wet, fluctuating climate produced by the gradual transition from a fluvial to an estuarine and marine setting that

characterizes the Springhill Formation," which seemed "not so stressing" for plants. Following these considerations, and taking into account the details of the layers examined herein, this suggestion seems to be in agreement with an adaptation to a "not so stressing" environment for the following reasons:

1. The absence of a polylamellate A1 layer, considered very protective and even related with xeric environments (Guignard et al., 2017; Yang et al., 2018).

2. A small proportion of granular layers (A2 and B2). The A2 layer was 8.96% - 19.86% of the total CM, and it was observed in 4 of the 6 types of cuticles. The B2 layer was 16.41% - 24.05% of the total CM, and it was observed in 2 of the 6 types of cuticles.

3. A high proportion of fibrillar B1 layer (61.53% - 100% of the total CM, and it was observed in all of the 6 cuticles).

The two latter remarks -a small proportion of granular layers (A2 and B2) and a much higher proportion of B1 layer- could be, according to a very cautious interpretation, an indication of at least, a "not so stressing" palaeoenvironment. This conclusion is in accordance with other previous papers with the former comparisons between two localities with the same taxon of fossil Cheirolepidiaceae (Yang et al., 2018), and two fossil taxa of Ginkgolaes in different localities (Del Fueyo et al., 2013; Guignard et al., 2016). In living plants, like the conifer *Pinus halepensis* (Aleppo pine) from Italy (Bartiromo et al. 2012), the leaf cuticles of the same taxon growing under volcanic gas fumigation (= very stressing environment) or not (= not stressing environment) were analyzed. Although unsignificant thickness variations of the cell wall plus cuticle of both fumigated and non-fumigated leaves have been found, a significant variation in the proportions of the cell wall and total cuticle thickness

between the two environments were observed, especially in the proportions between the three zones of B1 fibrillar layer. This ultrastructure study in *P. halepensis* demonstrated the very intimate influence of the environment versus taxonomy characters. Conversely, concerning EDS elements and taking into consideration that sulfur is extremely present in the volcanic atmosphere, no sulfur was found in both types of cuticles, demonstrating (at least for this element) an absence of environmental influence. However, we have to be cautious as 1/ it was the only element analyzed and 2/ it is the only comparison in living gymnosperm which is actually a very large group.

The micropalaeoenvironment (Guignard, 2019) may also be enhanced to a certain point, which may be summarized as the environment differences just adjacent to a plant or a leaf (between the upper part and the lower part of leaf; including upper and lower cuticles). Although it was properly demonstrated in detail for two types of cuticles of *Komlopteris nordenskioeldii* (Nathorst) Barbacka of Pteridospermales (Guignard et al., 2001), it seems to be much less evident for the present *Ptilophyllum* study. Thanks to statistical measurements (table 1), it was found that the cuticular membranes' thicknesses of the two upper and lower ordinary epidermal cell cuticles are different; the first one is significantly thicker, having been more exposed to the sun, rain and wind; while the second one, which is thinner, lies more protected. However, the details of the cuticles do not follow the equilibrium of granules and fibrils evocated above for the macropalaeoenvironment; other factors were probably involved in these cuticles.

5.4.1 EDS and Taxonomy

Firstly, the only S/Ca ratio considered for statistical purposes reveals a very special identity for *Ptilophyllum eminelidarum*. In former studies, the selected ratios were 3-5, and the elements 4-5 (Guignard et al., 2016, 2017, 2019; Yang et al., 2018); exceptionally, they amounted to 10 ratios and 6 elements for one study (Carrizo et al., 2019b).

Chemical elements are of great interest for the insights about cuticles, e.g., in chemotaxonomy (D'Angelo and Zodrow, 2018; D'Angelo and Zodrow, 2022). In most of the few studies conducted on cuticle elements, S and/or Ca were present. In fact, they were present in the following cases: in Coniferales, in Cheirolepidiaceae, Ca in *Suturovagina intermedia* Chow et Tsao (Yang et al., 2018), S in *Pseudofrenelopsis dalatzensis* (Chow et Tsao) Cao ex Zhou and in *P. gansuensis* Deng, Yang et Lu (Guignard et al., 2017); in Araucariaceae, S and Ca in *Brachyphyllum garciarum* (Carrizo et al., 2019b); in Ginkgoales, S and Ca in *Ginkgoites ticoensis* Archangelsky, in *G. skottsbergii* Lundblad (Guignard et al., 2016); and in *Baiera furcata* (Lindley et Hutton) Braun (Guignard et al., 2019).

Specifically, only *Ginkgoites ticoensis* and *G. skotttsbergii* (Guignard et al., 2016), and *Brachyphyllum garciarum* (Carrizo et al., 2019b), present the S/Ca significant ratio, facilitating a distinction between layers of cuticles- "only" for the A2 and B1 layers of the upper cuticle in *B. garciarum* (their table 3). Moreover, the lowest reliable ratio among 10 ratios in total "only" occurs between the two A1 layers of the *Ginkgoites* species (their table 3), the A2 and B1 layers being homogeneous (= with unsignificant differences) in these two species, for a total of 5 ratios in this study. Besides enhancing the identity of this taxon by the insignificant values of S and Ca within the two types of upper and lower cuticles, the present study of *Ptilophyllum*, with homogeneous values of S/Ca among all layers (Fig. 1, Appendix G), emphasizes

nonetheless, once more, the little significance of this ratio among the layers of cuticles. As this is the first elements EDS study so far in Bennettitales, it is still questionable whether this ratio is of species, genus, family or order taxonomical signature; however, it must be noticed that the S/Ca ratios values of other previously studied taxa, which belong to other families/orders, are different. *Ptilophyllum eminelidarum* has the lowest ratio (0-0.56), *B. garciarum* (Araucariaceae) being 5.38-22.98, *Ginkgoites* species (Ginkgoales) with *G. skottsbergii* being 6.53-17.45 and *G. ticoensis* having values of 2.95-56.45. Certainly, EDS parameters should be checked within the same species collected from different localities to test the putative influence of the environment on EDS elements.

As the A1 layer is absent in the *Ptilophyllum eminelidarum* cuticle, the homogeneity of the ratios among A2, B1, and B2 layers may be a little excessive, but potentially reveals the identity of the taxon. Moreover, it is at least in agreement with the previous remark highlighted in the study of *Brachyphyllum garciarum* (Carrizo et al., 2019b). In this taxon, the A1 layer was proved to be an element of distinction between genera or species, as in other taxa, for instance, gymnosperms, seed ferns, conifers and cycad-related fossils, and pteridophyll cuticles (Zodrow and Mastalerz, 2007; D'Angelo et al., 2010; Zodrow et al., 2010; D'Angelo et al., 2011; D'Angelo and Zodrow, 2011; D'Angelo et al., 2012).

5.4.2 EDS and the Palaeoenvironment

The characterization of the chemical elements of the environment of a plant *sensu lato* of the cuticle has gradually became of interest (He et al., 2018; Hu et al., 2023), especially in agronomy (Sarkar et al., 2023). S was studied in cuticles, though

much less than Ca. In living angiosperms, such as *Robinia pseudoacacia* L., Rashidi et al. (2012) found that SO_2, among other atmospheric pollutants, made the upper cuticle of the leaf thicker. In a study of acid rain in *Liquidambar styraciflua* L. and in *Fraxinus uhdei* (Wenz.), Lingelsh Rodríguez-Sánchez et al. (2020) revealed that an experimental pH 2.5 by sulfuric acid causes "cuticle alterations…". On the other hand, the importance for S in fossil cuticles was indicated in Ginkgoales and Bennettitales (Steinthorsdottir et al., 2018).

In contrast, the content of Ca in cuticles has been far more studied. Smalley et al. (1993), demonstrated that the use of solutions with both S and Ca, among other chemicals, changes the permeability of the cuticles in living *Pyrus communis* L. and in *Citrus limon* (L.) Burm. Fils cv Ponderosa. The utmost importance of calcium oxalate (CaOx) in fossil and living plant leaves was indicated by Melekhosseini et al. (2022). However, it should be noticed that these crystals represent very concentrated amounts of Ca that are not homogeneously dispersed throughout the cuticle layers, as is the case in the fossil *Ptilophyllum eminelidarium*. The same occurs in the living *Picea abies* (L.) H. Karst, where these crystals of Ca were detected in a "layer-like" fashion through Confocal Raman microscopy (Sasani et al., 2021). Ca was also largely studied in horticulture, e.g., in living fruits of *Prunus cerasus* L. and cultivars (Winkler et al., 2020; Winkler and Knoche, 2019; Winkler and Knoche, 2021), in fruits of *Vitis vinifera* L. and cultivars (Martins et al., 2020), and in fruits of *Citrus sinensis* (L.) Osbeck and cultivars (Bonomelli et al., 2022). The latter study provided some TEM sections of the fruit cuticles but failed to show any details of the cuticle layers.

Unfortunately, none of these articles relate the details of the element contents. However, the content of Ca was thoroughly studied in cuticles in relation to xerothermy and stress (Guzman-Delgado et al., 2016). In a study of living *Arabidopsis thaliana* (L.)

Heynh. leaves, Benikhlef et al (2013) experimented what they called "a soft mechanical stimulation", inducing artificial "stress" accomplished by means of a higher Ca content. Following these remarks regarding the sensitivity to the environment, in recent studies of detailed layers of fossil cuticles and at different levels of comparisons, Ca was putatively related with xerothermy. For example, in Cheirolepidiaceae (Yang et al., 2018), two localities where the same taxon had been collected were compared. Also, Ca was related with xerothermy in a comparison between two species in Ginkgoales (Guignard et al., 2019). Additionally, Ca was putatively related with stress in a comparison between upper and lower cuticles of one taxon of Araucariaceae (Carrizo et al., 2019b).

As the results of the present study are the first detailed EDS data obtained in cuticles among Bennettitales, we must be extremely cautious when making palaeoenvironmental comparisons with other taxa, given that, at this stage, the relationship between S/Ca and the palaeoenvironment seems fairly weak. For *Brachyphyllum garciarum*, the S/Ca was significant (Carrizo et al., 2019b), in contrast with that obtained for *Ptilophyllum eminelidarum*, which was collected in the same fossiliferous locality (5.32-22.98 versus 0-0.56, respectively). The S/Ca ratio for *Ginkgoites skottsbergi* (Guignard et al., 2016) was in the same range as that of *B. garciarum* (6.53-17.45), although both taxa belong to different palaeoenvironments. Nevertheless, 1. the only putative relationship found with S could be with *G. ticoensis* (Del Fueyo et al., 2013) from a volcanic area, and with the highest S/Ca ratio (S/Ca ratio was 2.95-56.45); while the present *Ptilophyllum eminelidarum* with the lowest S/Ca ratio was not from a volcanic area; 2. compared with *B. garciarum* (Carrizo et al., 2019b), as the S/Ca ratios values were not significantly different between upper and

lower cuticles in *Ptilophyllum eminelidarum*, a putative similar influence of the palaeoenvironment on these two opposite parts of the leaf can be assumed.

6. Conclusion

In *Ptilophyllum eminelidarum,* the TEM ultrathin 60 to 70-nanometer sections facilitate the identification of 6 types of cuticles, i.e., upper and lower ordinary epidermal cell cuticles, subsidiary and guard cell cuticles of the stomatal apparatus, and simple and compound papilla cuticles. The two first types are made with an A2 granular layer of the cuticle proper, a B1 fibrillar layer, and a B2 granular layer of the cuticular layer. This corresponds to the former brief TEM study where this taxon was erected (Carrizo et al., 2019a). Such a characterization reinforces the uniqueness of this case compared with all other taxa formerly studied; it could be the basis for erecting Bennettitales as a heterogeneous group of cuticles (Guignard, 2019). The stomatal apparatus cuticles are made with a B1 layer, while the papillae are made with A2 and B1 layers. All said details were observed in the majority of cases and allow us to obtain the most accurate synthesis with statistical measurements; however, this material is characterized by a certain degree of complexity, and other combinations also occur in all of the six types of cuticles.

According to a factorial component analysis, the hierarchy of the types of cuticles is as follows: subsidiary and guard cell cuticles of the stomatal apparatus, then both epidermal cell cuticles, and finally, both papillae cuticles. The above described hierarchy enhances the great interest evoked by the stomatal apparatus versus the little interest raised by epidermal cell cuticles. Student's t-tests reveal, for all cuticles, a high level of independence when compared between one another: 60-87% for their thickness

values, and 57.5-100% for their thickness percentages, indicating the individuality and interest of each cuticle.

For the 9 variables studied in the factorial component analysis, the hierarchy is as follows: means B2 and A2 for the first set of layers, then B1%, CL%, and mean B1 for the second set; finally, B2%, A2%, mean CL, and mean CM for the third set. For their thickness values, their independence was less variable (73-87%), while for their thickness percentages it was more variable: 0-87%. The 5 most important variables (means B2 and A2, B1 and CL %, and mean B1) are, at the same time, the most independent (mean of 83.5%), versus the 4 less important variables cuticles (B2 and A2%, means CL and CM), which are the less independent (mean of 57.25%). Such reasoning could be used as a criterion for the preference of the first variables for identification in Bennettitales.

Based on the complementarity among the 9 variables and the 6 types of cuticles, the results obtained in multidimensional analyses (factorial and hierarchical component analyses), and Student's t-tests, a dichotomous key was built, which proved very useful in a laboratory identification work, where the identification of each of the 6 types of cuticles was possible based on very few variables.

Considering the details of layers and the palaeoenvironment, the present detailed TEM results seem to show, in a very cautious assumption (as comparisons with other taxa from other macropalaeoenvironments were lacking) that the present *Ptilophyllum eminelidarum* was living in a "not so stressing" locality. Such an assumption was built on account of the absence of an A1 polylamellate layer, a small proportion of granular layers (A2 and B2 layers), and a high proportion of fibrils (B1 layer). The micropalaeoenvironment can be evocated too; the cuticular membranes' thicknesses of the two upper and lower ordinary epidermal cell cuticles are different: the first one,

significantly thicker, appears to have been typically more exposed to the sun, rain and wind while the second one, which is thinner, was more protected.

The elements EDS values reveal an homogeneous S/Ca ratio for all layers of upper and lower cuticles. The taxonomical discussion reveals the identity of *Ptilophyllum eminelidarum*. Palaeoenvironmental considerations lead to making assumptions with extreme precaution; at least S/Ca ratios values were found not to be significantly different between upper and lower cuticles; a putative similar influence of the palaeoenvironment on these two opposite parts of the leaf can be presumed, at least for these elements.

As these are the first detailed statistical TEM and EDS studies in Bennettitales, they may be useful in the future as a basis for further comparisons in the same group, and will reinforce or modulate the above-mentioned characteristics, at the species, genus or higher taxonomical level, highlighting the great interest of detailed TEM studies and the potential interest of each type of cuticle and layer, instead of just providing the total thickness of the cuticular membrane.

Special dedication

As the present special issue is devoted to Prof. Archangelsky who was one of the pioneers of TEM ultrastructure studies in fossil plants, here is the copy of the electronic message (very slightly corrected for writing mistakes) to G. Guignard received from Prof. Archangelsky on 15th november 2019, as a reply to the online appearance of his review article in the special issue “Plant cuticles, fine details” (Guignard et al., 2021).

Dear Dr. Guignard,

Thank you for sending me a copy of your RPP article. It shows how useful TEM microscopy with fossils may be.

Originally, I was encouraged in the eighties while visiting Tom Taylor at Ohio State University with a British Council Scholarship. I had at my disposal a nice TEM microscope and made useful my time by sectioning excellent cuticnized material that was studied earlier with the guidance of Tom Harris at Reading University. At that time I also visited R. Florin and E. Boureau.

Back in Argentina I had the chance to share my experiences in Tucuman University (and also La Plata Nat. Hist. Museum students). I am glad to see the progress in these studies in different countries: it is a new world for paleobotanical research.

At present, I have retired and doing some writing at home, mainly personal aspects of my researches, a sort of Memoires.

Thank you for the letter and the copy of your article.

Yours sincerely

Sergio Archangelsky

Acknowledgments

This paper is a contribution to grants ANPCYT PICT 2020/2271, ANPCyT PICT 2021/158 and CONICET PIP 112-202101-00016**.** We wish to thank the technical staff of the University Lyon 1 «centre technologique des microstructures CTμ", especially Xavier Jaurand, Charline Dalverny, Lucie Geay and Anton Sak for improvement of the study. We are grateful to Natalia Zavialova and the anonymous reviewer for all their valuable comments, which have undoubtedly improved the quality of the manuscript.

References

Archangelsky, A., Andreis, R.R., Archangelsky, S., Artabe, A., 1995. Cuticular Characters Adapted to Volcanic Stress in a New Cretaceous Cycad Leaf from Patagonia, Argentina - Considerations on the Stratigraphy and Depositional History of the Baqueró Formation. Review of Palaeobotany and Palynology 89, 213-233.

Archangelsky, S., 1976. Vegetales fósiles de la Formación Springhill, Cretácico, en el subsuelo de la Cuenca Magallánica, Chile. Ameghiniana 13, 141-158.

Archangelsky, S., Archangelsky, A., 2004. Palinología estadística en el Cretácico de la Cuenca Austral, Plataforma Continental Argentina. II. Seis perforaciones del área Gallegos. III. Discusión y conclusiones. Revista del Museo Argentino de Ciencias Naturales (Nueva Serie) 6 245-255.

Archangelsky, S., Baldoni, A., 1972. Revisión de las Bennettitales de la Formación Baqueró (Cretácico Inferior) provincia de Santa Cruz. I. Hojas. Revista Museo de La Plata (Nueva Serie) Paleontología 7, 195-265.

Archangelsky, S., Taylor, T.N., 1986. Ultrastructural Studies of Fossil Plant Cuticles. 2. Tarphyderma Gen-N, a Cretaceous Conifer from Argentina. American Journal of Botany 73, 1577-1587.

Archangelsky, S., Taylor, T.N., Kurmann, M.H., 1986. Ultrastructural Studies of Fossil Plant Cuticles - *Ticoa harrisii* from the Early Cretaceous of Argentina. Botanical Journal of the Linnean Society 92, 101-116.

Artabe, A.E., Zamuner, A.B., Archangelsky, S., 1991. Estudios cuticulares en Cycadópsidas fósiles. El género *Kurtziana* Frenguelli 1942. Ameghiniana 28, 365-374.

Baldoni, A.M., 1979. Nuevos elementos paleoflorísticos de la tafoflora de la Formación Spring Hill, limite Jurásico-Cretácico subsuelo de Argentina y Chile Austral. Ameghiniana 16, 103-119.

Baldoni, A.M., Taylor, T.N., 1983. Plant remains from a new Cretaceous site in Santa Cruz, Argentina. Review of Palaeobotany and Palynology 39, 301-311.

Barale, G., Baldoni, A.M., 1993. L'ultrastructure de la cuticule de quelques Bennettitales du Crétacé inférieur d'Argentine. Comptes Rendues de l'Académie des Sciences de Paris 316, 1171-1177.

Bartiromo, A., Guignard, G., Lumaga, M.R.B., Barattolo, F., Chiodini, G., Avino, R., Guerriero, G., Barale, G., 2012. Influence of volcanic gases on the epidermis of Pinus halepensis Mill. in Campi Flegrei, Southern Italy: A possible tool for detecting volcanism in present and past floras. Journal of Volcanology and Geothermal Research 233, 1-17.

Bartiromo, A., Guignard, G., Lumaga, M.R.B., Barattolo, F., Chiodini, G., Avino, R., Guerriero, G., Barale, G., 2013. The cuticle micromorphology of in situ *Erica*

arborea L. exposed to long-term volcanic gases. Environmental and Experimental Botany 87, 197-206.

Benikhlef, L., L'Haridon, F., Abou-Mansour, E., Serrano, M., Binda, M., Costa, A., Lehmann, S., Métraux, J.P., 2013. Perception of soft mechanical stress in *Arabidopsis* leaves activates disease resistance. BMC Plant Biology 13, 133.

Berhin, A., Nawrath, C., Hachez, C., 2022. Subtle interplay between trichome development and cuticle formation in plants. New Phytologist 233, 2036-2046.

Bock, P., Felhofer, M., Mayer, K., Gierlinger, N., 2021. A Guide to elucidate the hidden multicomponent layered structure of plant cuticles by Raman Imaging. Frontiers in Plant Science 12.

Bonomelli, C., Fernandez, V., Capurro, F., Palma, C., Videla, X., Rojas-Silva, X., Nario, A., Martiz, J., 2022. Absorption and distribution of Calcium (Ca-45) applied to the surface of orange (*Citrus sinensis*) fruits at different developmental stages. Agronomy 12, 150.

Brongniart, A.T., 1834 Nouvelles recherches sur la structure de l'épiderme des végétaux. Annales des Sciences Naturelles, Botanique 2nd ser. 1, 65-71.

Bueno, A., Alonso-Forn, D., Peguero-Pina, J.J., de Souza, A.X., Ferrio, J.P., Sancho-Knapik, D., Gil-Pelegrín, E., 2022. Minimumv leaf conductance (gmin) is higher in the treeline of *Pinus uncinata* Ram. in the Pyrenees: Michaelis; Hypothesis Revisited. Frontiers in Plant Science 12, 786933.

Carrizo, M.A., Del Fueyo, G.M., 2015. The Early Cretaceous megaflora of the Springhill Formation, Patagonia. Paleofloristic and Paleonvironmental inferences. Cretaceous Research 56, 93-109.

Carrizo, M.A., Del Fueyo, G.M., Medina, F., 2014. Foliar cuticle of *Ruflorinia orlandoi* nov. sp. (Pteridospermophyta) from the Lower Cretaceous of Patagonia. Geobios 47, 87-99.

Carrizo, M.A., Lafuente Diaz, M.A., Del Fueyo, G.M., 2019a. Resolving taxonomic problems through cuticular analysis in Early Cretaceous bennettitalean leaves from Patagonia. Cretaceous Research 97, 40-51.

Carrizo, M.A., Lafuente Diaz, M.A., Del Fueyo, G.M., Guignard, G., 2019b. Cuticle ultrastructure in *Brachyphyllum garciarum* sp. nov (Lower Cretaceous, Argentina) reveals its araucarian affinity. Review of Palaeobotany and Palynology 269, 104-128.

Cleal, C.J., Zodrow, E.L., 1989. Epidermal structure of some medullosan Neuropteris foliage from the Middle and Upper Carboniferous of Canada and Germany Palaeontology 32, 837-882.

Cortiñas, J.C., Artabe, H.A., 1981. Un nuevo afloramiento fosilífero de la Formación Springhill, en el Noroeste de la provincia de Santa Cruz. Revista de la Asociación Geológica Argentina 36, 212-214.

D'Angelo, J.A., Zodrow, E.L., 2011. Chemometric study of functional groups in different layers of *Trigonocarpus grandis* ovules (Pennsylvanian seed fern, Canada). Organic Geochemistry 42, 1039-1054.

D'Angelo, J.A., Zodrow, E.L., 2018. Fossil cutin of *Johnstonia coriacea* (Corystospermaceae, Upper Triassic, Cacheuta, Argentina). International Journal of Coal Geology 189, 70-74.

D'Angelo, J.A., Zodrow, E.L., 2022. Chemotaxonomic comparison of the seed ferns *Odontopteris cantabrica* and *Odontopteris schlotheimii*, Middle Pennsylvanian Sydney Coalfield, Canada. Lethaia 55, 1-8.

D'Angelo, J.A., Zodrow, E.L., Camargo, A., 2010. Chemometric study of functional groups in Pennsylvanian gymnosperm plant organs (Sydney Coalfield, Canada): Implications for chemotaxonomy and assessment of kerogen formation. Organic Geochemistry 41, 1312-1325.

D'Angelo, J.A., Zodrow, E.L., Mastalerz, M., 2012. Compression map, functional groups and fossilization: A chemometric approach (Pennsylvanian neuropteroid foliage, Canada). International Journal of Coal Geology 90, 149-155.

D'Angelo, J.A., Escudero, L.B., Volkheimer, W., Zodrow, E.L., 2011. Chemometric analysis of functional groups in fossil remains of the *Dicroidium* flora (Cacheuta, Mendoza, Argentina): Implications for kerogen formation. International Journal of Coal Geology 87, 97-111.

Del Fueyo, G.M., Villar de Seoane, L., Archangelsky, S., Guignard, G., 2006. Estudios cuticulares de *Ginkgoites* Seward del Cretácico Inferior de Patagonia. Revista del Museo Argentino de Ciencias Naturales 8, 143–149.

Del Fueyo, G.M., Guignard, G., Villar de Seoane, L., Archangelsky, S., 2013. Leaf cuticle anatomy and the ultrastructure of *Ginkgoites ticoensis* Archang. from the Aptian of Patagonia. International Journal of Plant Sciences 174, 406-424.

Florin, R., 1958. On Jurassic taxads and conifers from north-western Europe and eastern Greenland. Acta Horti Bergiani 17 259-402.

Giacosa, R., Franchi, M., 2001. Hojas Geológicas 4772-III y 4772-IV Lago Belgrano y Lago Posadas, Provincia de Santa Cruz. Buenos Aires Servicio Geológico Minero Argentino. Instituto de Geología y Recursos Minerales.

González-Valenzuela, L., Renard, J., Depège-Fargeix, N., Ingram, G., 2023. The plant cuticle. Current Biology 33, R210-R214.

Guignard, G., 2019. Thirty-three years (1986-2019) of fossil plant cuticle studies using transmission electron microscopy: A review. Review of Palaeobotany and Palynology 271, 104097.

Guignard, G., 2021. Method for ultrastructural fine details of plant cuticles by transmission electron microscopy. MethodsX 8, 101391.

Guignard, G., Zhou, Z., 2005. Comparative studies of leaf cuticle ultrastructure between living and the oldest known fossil Ginkgos in China. International Journal of Plant Sciences 166, 145-156.

Guignard, G., Thevenard, F., van Konijnenburg-van Cittert, J.H.A., 1998. Cuticle ultrastructure of the cheriolepidiaceous conifer *Hirmeriella muensteri* (Schenk) Jung. Review of Palaeobotany and Palynology 104, 115-141.

Guignard, G., Popa, M.E., Barale, G., 2004. Ultrastructure of Early Jurassic fossil plant cuticles: *Pachypteris gradinarui* Popa. Tissue Cell 36, 263-273.

Guignard, G., Boka, K., Barbacka, M., 2001. Sun and shade leaves? Cuticle ultrastructure of Jurassic *Komlopteris nordenskioeldii* (Nathorst) Barbacka. Review of Palaeobotany and Palynology 114, 191-208.

Guignard, G., Del Fueyo, G.M., Villar de Seoane, L., Carrizo, M.A., Lafuente Diaz, M.A., 2016. Insights into the leaf cuticle fine structure of *Ginkgoites skottsbergii* Lundblad from the Albian of Patagonia and its relationship within Ginkgoaceae. Review of Palaeobotany and Palynology 232, 22-39.

Guignard, G., Yang, X.-J., Wang, Y.-D., 2017. Cuticle ultrastructure of *Pseudofrenelopsis gansuensis*: Further taxonomical implications for Cheirolepidiaceae. Cretaceous Research 71, 24-39.

Guignard, G., Yang, X.-J., Wang, Y.-D., 2019. Cuticle ultrastructure of *Baiera furcata* from Northeast China and its implication in taxonomy and paleoenvironment. Review of Palaeobotany and Palynology 268, 95-108.

Guignard, G., Zodrow, E.L., Del Fueyo, G.M., 2021. Plant cuticles, fine details. Review of Palaeobotany and Palynology 288, 104402.

Guzman-Delgado, P., Graca, J., Cabral, V., Gil, L., Fernandez, V., 2016. The presence of cutan limits the interpretation of cuticular chemistry and structure: *Ficus elastica* leaf as an example. Physiologia Plantarum 157, 205-220.

Harris, T.M., 1964. The Yorkshire Jurassic Flora II. Caytoniales, Cycadales & Pteridosperms British Museum (Natural History), London.

He, M., He, C.Q., Ding, N.Z., 2018. Abiotic stresses: general defenses of land plants and chances for engineering multistress tolerance. Frontiers in Plant Science 9, 1771.

Holloway, P.J., 1982. Structure and histochemistry of plant cuticular membranes: an overview, in: Cutler, D.F., Alvin, K.L., Price, C.E. (Eds.), The Plant Cuticle Linnean Society London, 1-32.

Hu, Y., Bellaloui, N., Kuang, Y., 2023. Editorial: Factors affecting the efficacy of foliar fertilizers and the uptake of atmospheric aerosols, volume II. Frontiers in Plant Science 14, 1146853.

Kerp, H., 1990. The study of fossil Gymnosperms by means of cuticular analysis. Palaios 5, 548-569.

Lafuente Diaz, M.A., Carrizo, M.A., Del Fueyo, G.M., D'Angelo, J.A., 2019. Chemometric approach to the foliar cuticle of *Ptilophyllum micropapillosum* sp. nov. from the Springhill Formation (Lower Cretaceous, Argentina). Review of Palaeobotany and Palynology 271, 104110.

Liu, L., Wang, X.Y., Chang, C., 2022. Toward a smart skin: Harnessing cuticle biosynthesis for crop adaptation to drought, salinity, temperature, and ultraviolet stress. Frontiers in Plant Science 13, 961829.

Lugardon, B., 1971. Contribution à la connaissance de la morphogénèse et de la structure des parois sporales chez les Filicinées isosporées. Toulouse France.

Machado, S.R., Bento, K.B.D., Canaveze, Y., Rodrigues, T.M., 2023. Peltate trichomes in the dormant shoot apex of *Metrodorea nigra*, a Rutaceae species with rhythmic growth. Plant Biology 25, 161-175.

Malekhosseini, M., Ensikat, H.-J., McCoy, V.E., Wappler, T., Weigend, M., Kunzmann, L., Rust, J., 2022. Traces of calcium oxalate biomineralization in fossil leaves from late Oligocene maar deposits from Germany. Scientific Reports 12, 15959.

Martinez, L.C.A., Artabe, A.E., Archangelsky, S., 2020. Studies of the leaf cuticle fine structure of *Zuberia papillata* (Townrow) Artabe 1990 from Hoyada de Ischigualasto (Upper Triassic), San Juan Province, Argentina. Review of Palaeobotany and Palynology 281, 104272.

Martins, V., Garcia, A., Alhinho, A.T., Costa, P., Lanceros-Mendez, S., Costa, M.M.R., Geros, H., 2020. Vineyard calcium sprays induce changes in grape berry skin, firmness, cell wall composition and expression of cell wall-related genes. Plant Physiology and Biochemistry 150, 49-55.

Menéndez, C.A., 1966. Fossil Bennettitales from the Tico flora Santa Cruz Province, Argentina. Bulletin of the British Museum (natural History) Geology 12, 3-42.

Molina, I., Bueno, A., Heredia, A., Domínguez, E., 2023. Editorial: Plant cuticle: From biosynthesis to ecological functions. Frontiers in Plant Science 14, 1154255.

Nosova, N., Yakovleva, O., Ivanova, A., Kiritchkova, A., 2016. First data on the ultrastructure of the leaf cuticle of a Mesozoic conifer, *Mirovia reymanowna* (Miroviaceae). Review of Palaeobotany and Palynology 233, 115-124.

Nosova, N., Yakovleva, O., Kotina, E., 2019. First data on the leaf cuticle ultrastructure of the Mesozoic genus Pseudotorellia Florin. Review of Palaeobotany and Palynology 271, 104096.

Oldham, T.C.B., 1976. Flora of the Wealden plant debris beds of England Palaeontology 19 437-502.

Ottone, E.G., Aguirre-Urreta, M.B., 2000. Palinomorfos cretacicos de la Formación Springhill en Estancia El Salitral, Patagonia Austral, Argentina Ameghiniana 37, 375-378.

Paiva, E.A.S., Oliveira, D.M.T., Canaveze, Y., Machado, S.R., 2022. Adhesive secretion in *Schizolobium parahyba* (Vell.) Blake (Leguminosae: Caesalpinioideae): histochemical and morpho-functional characterization of this unusual feature in woody plants. Arthropod-Plant Interactions 16, 249-261.

Passalia, M.G., Del Fueyo, G., Archangelsky, S., 2010. An Early Cretaceous zamiaceous cycad of South West Gondwana: *Restrepophyllum* nov. gen. from Patagonia, Argentina. Review of Palaeobotany and Palynology 161, 137-150.

Philippe, G., De Bellis, D., Rose, J.K.C., Nawrath, C., 2022. Trafficking processes and secretion pathways underlying the formation of plant cuticles. Frontiers in Plant Science 12, 786874.

Rashidi, F., Jalili, A., Kafaki, S.B., Sagheb-Talebi, K., Hodgson, J., 2012. Anatomical responses of leaves of Black Locust (*Robinia pseudoacacia* L.) to urban pollutant gases and climatic factors. Trees - Structure and Function 26, 363-375.

Reynoud, N., Geneix, N., Petit, J., D'Orlando, A., Fanuel, M., Marion, D., Rothan, C., Lahaye, M., Bakan, B., 2022. The cutin polymer matrix undergoes a fine architectural tuning from early tomato fruit development to ripening. Plant Physiology, 190, 1821-1840.

Reynoud, N., Petit, J., Bres, C., Lahaye, M., Rothan, C., Marion, D., Bakan, B., 2021. The Complex Architecture of Plant Cuticles and Its Relation to Multiple Biological Functions. Frontiers in Plant Science 12, 782773.

Riccardi, A.C., 1976. Paleontología y edad de la Formación Springhill Primer Congreso Geológico Chileno, 1. Santiago, Chile, C41-C56.

Richardson, K.C., Jarett, L., Finke, E.H., 1960. Embedding in Epoxy resins for ultrathin sectioning in electron microscopy. Stain Technology 35, 313-323.

Rodríguez-Sánchez, V.M., Rosas, U., Calva-Vasquez, G., Sandoval-Zapotitla, E., 2020. Does acid rain alter the leaf anatomy and photosynthetic pigments in urban trees? Plants 9, 862.

Sarkar, S., Arya, G.C., Negin, B., Manasherova, E., Levy, M., Aharoni, A., Cohen, H., 2023. Compositional variances in cuticular lipids of wild and domesticated barley leaves and their impact on plant-environment interactions. Environmental and Experimental Botany 206, 105140.

Sasani, N., Bock, P., Felhofer, M., Gierlinger, N., 2021. Raman imaging reveals in-situ microchemistry of cuticle and epidermis of spruce needles. Plant Methods 17, 17.

Situngu, S., Barker, N.P., 2022. A comparative study of the anatomy of leaf domatia in *Gardenia thunbergia* Thunb., *Rothmannia capensis* Thunb., and *Rothmannia globosa* (Hochst.) Keay (Rubiaceae). Plants 11, 3126.

Smalley, S.J., Hauser, H.D., Berg, V.S., 1993. Effect of cations on effective permeability of leaf cuticles to sulfuric acid. Plant Physiology 103, 251–256.

Spalleti, L.A., Schwarz, E., Veiga, G.D., Matheos, S.D., Haring, C., Covellone, G., 2009. Análisis paleoambiental y estratigráfico secuencial de alta resolución de la Formación Springhill al este de Tierra del Fuego (Cuenca Austral, Argentina) XII Congreso Geológico Chileno, Santiago Actas, 1-4.

Steinthorsdottir, M., Elliott-Kingston, C., Bacon, K.L., 2018. Cuticle surfaces of fossil plants as a potential proxy for volcanic SO2 emissions: observations from the Triassic-Jurassic transition of East Greenland. Palaeobiodiversity and Palaeoenvironments 98, 49-69.

Taylor, T.N., Taylor, E.L., Krings, M., 2009. Palaeobotany the biology and Evolution of fossil plants. Second Edition. Academic Press, Burlington, MA.

Thevenard, F., Barale, G., Guignard, G., Daviero-Gomez, V., Gomez, B., Philippe, M., Labert, N., 2005. Reappraisal of the ill-defined Liassic pteridosperm *Dichopteris* using an ultrastructural approach. Botanical Journal of the Linnean Society 149, 313-332.

Thomas, C.R., 1949. Manantiales Field, Magallanes Province, Chile. American Association of Petroleum Geologists 33, 1579–1589.

Villar de Seoane, L., 1995. Estudio cuticular de nuevas Bennettitales eocretacicas de Santa Cruz, Argentina, VI Congreso Argentino de Paleontologia y Bioestratigraphica, Actas, 247-254.

Villar de Seoane, L., 1999. *Otozamites ornatus* sp nov., a new bennettitalean leaf species from Patagonia, Argentina. Cretaceous Research 20, 499-506.

Villar de Seoane, L., 2001. Cuticular study of Bennettitales from the Springhill Formation, Lower Cretaceous of Patagonia, Argentina. Cretaceous Research 22, 461-479.

Villar de Seoane, L., 2003. Cuticle ultrastructure of the Bennettitales from the Anfiteatro de Tico Formation (Early Aptian), Santa Cruz Province, Argentina. Review of Palaeobotany and Palynology 127, 59-76.

Wang, X.Y., Chang, C., 2022. Exploring and exploiting cuticle biosynthesis for abiotic and biotic stress tolerance in wheat and barley. Frontiers in Plant Science 13, 1064390.

Wang, Y.D., Guignard, G., Thevenard, F., Dilcher, D., Barale, G., Mosbrugger, V., Yang, X.J., Mei, S.W., 2005. Cuticular anatomy of *Sphenobaiera huangii* (Ginkgoales) from the Lower Jurassic of Hubei, China. American Journal of Botany 92, 709-721.

Winkler, A., Fiedler, B., Knoche, M., 2020. Calcium physiology of sweet cherry fruits. Trees-Struct Funct 34, 1157-1167.

Winkler, A., Knoche, M., 2019. Calcium and the physiology of sweet cherries: A review. Scientia Horticulturae 245, 107-115.

Winkler, A., Knoche, M., 2021. Calcium uptake through skins of sweet cherry fruit: Effects of different calcium salts and surfactants. Scientia Horticulturae 276, 109761.

Yang, X.J., Guignard, G., Thevenard, F., Wang, Y.D., Barale, G., 2009. Leaf cuticle ultrastructure of *Pseudofrenelopsis dalatzensis* (Chow et Tsao) Cao ex Zhou (Cheirolepidiaceae) from the Lower Cretaceous Dalazi Formation of Jilin, China. Review of Palaeobotany and Palynology 153, 8-18.

Yang, X.J., Guignard, G., Zhou, Z.Y., Xu, Q., 2018. *Suturovagina intermedia* (Cheirolepidiaceae) from the Lower Cretaceous Dalazi Formation of Wangqing, Northeast China: Cuticle ultrastructure and palaeoenvironmental insights. Cretaceous Research 91, 80-99.

Zhou, Z.Y., Guignard, G., 1998. Leaf cuticle ultrastructure of two czekanowskialeans from the middle Jurassic Yima formation of Henan, China. Review of Palaeobotany and Palynology 102, 179-187.

Zodrow, E.L., D'Angelo, J.A., Mastalerz, M., Cleal, C.J., Keefe, D., 2010. Phytochemistry of the fossilized-cuticle frond *Macroneuropteris macrophylla* (Pennsylvanian seed fern, Canada). International Journal of Coal Geology 84, 71-82.

Zodrow, E.L., Mastalerz, M., 2007. Functional groups in a single pteridosperm species: Variability and circumscription (Pennsylvanian, Nova Scotia, Canada). International Journal of Coal Geology 70, 313-324.

Captions of plates and appendices

Plate I. Light microscopy, gross morphology and detail of epidermal cells and stomatal apparatus cuticles. Cp: compound papilla; Sp: simple papilla; Sc: subsidiary cell; St: stomatal apparatus. MPM-PB 15347-15348.

Fig. 1. Location map showing the Río Correntoso locality (red dot), Santa Cruz Province, Argentina.

Fig. 2. General aspect of the leaves and the leaflets.

Fig. 3. General aspect of lower epidermis showing the distribution of the compound and simple papillae.

Fig. 4-5. Details of stomatal apparatuses, simple papillae and compound papillae.

Fig. 6. Detail of ordinary cells of the upper epidermis, arrow shows detail of sinuous anticlinal walls.

Plate II. Scanning electron microscopy, external and internal views of the epidermis. MPM-PB 15347-15348.

Fig. 1. General aspect of external lower epidermis showing rows of compound papillae (arrows) between the rows of simple papillae.

Fig. 2. General aspect of internal lower and upper epidermis showing the base cells cuticles of the compound papillae (arrows) between the stomatal apparatuses. Dot line marks the margin of both epidermises.

Fig. 3-4. Details of simple and compound papillae. Note the fusion of some of the papilla segments between neighbor's papillae.

Fig. 5. Detail of the inner view of ordinary cells cuticles of the upper epidermis. Arrow points to the sinuous anticlinal walls.

Fig. 6. Detail of the inner view of a stomatal apparatus showing the guard and subsidiary cells cuticles. Arrow marks the base cell of a simple papilla.

Plate III. Transmission electron microscopy, ordinary epidermal cell cuticle of upper cuticle

Fig. 1 General view with A2 granular layer of the cuticle proper, B1 fibrillar layer and B2 granular layer of the cuticular layer, as observed in the majority. Number 2 indicates the location of enlarged part in fig. 2, with artificial colors.

Fig. 2 Enlargement of fig. 1, with artificial colors enhancing granules of the A2 and B2 layers (dark blue), B1 fibrils (arrow) appearing in light blue color at the middle part of the cuticle.

Figs. 3-8, combinations of layers also observed, in minor proportions.

Fig. 3 General view, with only B1 fibrillar layer and B2 granular layer of the cuticular layer. Numbers 4 and 5 indicate the location of adjacent figs. 4 and 5.

Fig. 4 Enlargement of fig. 3, with artificial colors enhancing B1 fibrils (arrows), in light blue color up to the outermost part of the cuticle, some granules (dark blue) being however present.

Fig. 5 Enlargement of fig. 3, with artificial colors enhancing B2 granules (dark blue) in the innermost part of the cuticle.

Fig. 6 General view, with A2 granular layer of the cuticle proper and B1 fibrillar layer of the cuticular layer. Numbers 7 and 8 indicate the location of adjacent figs. 7 and 8.

Fig. 7 Enlargement of fig. 6, with artificial colors enhancing A2 granules (dark blue) in the outermost part of the cuticle.

Fig. 8 Enlargement of fig. 6, with artificial colors enhancing B1 fibrils (arrows), in light blue color at the innermost part of the cuticle.

Plate IV. Light and transmission electron microscopies, edges of leaves.

Figs. 1-3, Light microscopy. Different sections, at the edge (arrows) of leaves cuticles, showing the connection between thicker upper cuticle and thinner lower cuticle. Note

that the edge presents various curves and long anticlinal walls in this well-preserved region.

Figs. 4-13, transmission electron microscopy.

Figs. 4-7, one part of edge with very heterogeneous in thickness cuticle, long anticlinal wall (AW) and even cell location (CL), revealing with artificial colors (Fig. 5) a dark blue outer zone with a maximum of granules (belonging to A2 of the cuticle proper, enlarged in fig. 6) mixed with some rare long fibrils zone (arrows), and light-blue inner zone with condensed fibrils quite distributed parallel [belonging to B1 of the cuticular layer, enlarged in fig. 7 (arrows)]. Numbers 6 and 7 correspond to the location of the enlargements provided in figs. 6,7; photo 7 is divided in two interesting fragments of this part of the cuticle. In photo 5, some diagonal lines may be due to an artefact of the diamond knife but do not affect the interpretations of the structures.

Figs. 8-10, a detail of edge outer zone, apparently homogeneous (fig. 8) but revealing with artificial colors (figs. 9,10) an outermost granular zone (A2) and fibrillar zone (B1) just below. For fig. 9, number 10 corresponds to the location of the enlargement provided in fig. 10, with short fibrils interconnected and randomly distributed.

Figs. 11,12, another detail of edge with fibrils in an outer zone, showing in this case more clearly contrasted long fibrils (belonging to B1 layer, arrows) orientated in various directions and mixed with granules (belonging to A2). For Fig. 11, number 12 represents the location of the enlargement provided in fig. 12

Fig. 13, one detail of a zone in the middle part of an edge cuticle, with concentrated long fibrils (belonging to B1, arrow) arranged more or less parallel, mixed with granules (belonging to A2).

Plate V. Transmission electron microscopy, ordinary epidermal cell cuticle of lower cuticle

Figs. 1-5, general view (Fig. 1) and details of the different parts of the cuticle, as observed in the majority. It is made with A2 granular layer of the cuticle proper in the outer part, fibrillar B1 layer in the middle part and granular B2 layer in the lower part of the cuticular layer. Numbers in fig. 1 refer to the location of the enlargements provided in figs 2-5.

Figs. 6-11, other combinations of layers observed in a minor proportion.

Figs. 6,7, B1 and B2 layers of the cuticular layer (fig. 7 being with artificial colors with B1 fibrils in light blue and B2 granules in dark blue).

Figs. 8,9, A2-B1 layers or just B1 layer (fig. 9 being with artificial colors, A2 granules being in dark blue and B1 fibrils in light blue); in the middle part of the cuticle fibrils are visible (arrows), slightly contrasted and not so concentrated as in the outer or inner parts.

Figs. 10,11, just A2 layer. (Fig. 11 being with artificial colors, A2 granules being in this case light and dark blue). Some very parallel lines may appear in some places, actually due to an artefact of the diamond knife and different from the fibrils as in figs; 8,9.

Plate VI. Light and transmission electron microscopy, simple papillae cuticle of lower cuticle.

Figs. 1-3, Light microscopy. Different sections of simple papillae cuticles with very few (Figs. 1 and 3) or even no lobulated segments (Fig. 2).

Figs 4-10, transmission electron microscope.

Figs 4,5, General views of two simple papillae cuticles, small (Fig. 4) and big (Fig. 5). Numbers in fig. 5 refer to the location of the enlargements provided in figs 6-10.

Figs 6-8, details of the different parts of the cuticle, as observed in the majority (fig. 8 is similar to fig. 7 but with artificial colors). The cuticle is made with A2 granular layer (dark blue) of the cuticle proper in the outer part, fibrillar (arrows) B1 layer (light blue) in the middle and lower parts of the cuticular layer. In an edge (fig. 6), fibrils are orientated quite at random.

Figs 9,10, details of the different parts of the cuticle, as observed in a minor proportion (fig. 10 is similar to fig. 9 but with artificial colors). The cuticle is made with A2 granular layer (dark blue) of the cuticle proper in the outer part, fibrillar B1 layer (light blue) in the middle part and granular B2 layer (dark blue) of the cuticular layer in the lowermost part. Some very parallel lines may appear in some places, actually due to an artefact of the diamond knife and different from the fibrils as in figs. 7,8.

Plate VII. Light and transmission electron microscopy, compound papillae cuticle of lower cuticle.

Figs. 1-6, Light microscopy. Different sections of compound papillae cuticle making very various schemes of lobules, some being very complex (Figs. 1, 4). IP = inner part, OP = outer part of cuticle.

Figs 7-15, transmission electron microscope.

Figs 7-10, General view of one compound papilla cuticle (for fig. 7, numbers 8-10 represent the photos numbers of enlarged parts). For fig. 8, number 9 represents the photo number of enlarged detail in the adjacent photo).

Figs. 9, 13-15 represent the details of the majority of cuticles observed, with A2 granular layer of the cuticle proper in the outer part, fibrillar (arrows) B1 layer in the middle and lower parts of the cuticular layer. For photo 13, numbers 14-15 represent the photos numbers of enlargements of this cuticle.

Figs 10-12, details of the different parts of the cuticle, as observed in the minority (fig. 12 is similar to fig. 11 but with artificial colors). Arrows indicate fibrils. The cuticle is made with only fibrillar (arrows) B1 layer of the cuticular layer, with very various concentrations of fibrils, (even very) sparsely present (and more or less randomly orientated) in the middle and upper parts of the cuticle and revealed with artificial colours, or very concentrated, especially in the lower part (and orientated parallel to the inner surface of the cuticle.

Plate VIII. Transmission electron microscopy, stomatal apparatus and subsidiary cell cuticles details.

Figs. 1,2. Sections of stomatal apparatus, just below one compound papilla CP for fig. 1, where the outer OC and inner IC chambers are visible, also the two subsidiary cell cuticles SC, and one guard cell cuticle GC for this longitudinal section. Fig. 2 is a transversal section with two guard cell cuticles apparently not entire.

Figs. 3-13, details of subsidiary cell cuticle.

Figs. 3,4, 7-13 represent the details of the majority of cuticles observed, with only fibrillar (arrows) B1 layer of the cuticular layer. Figs. 7-9 are outermost parts of the cuticle, fig. 8 being similar to fig. 7 but with artificial colors. Figs. 12,13 are the middle part. Figs. 10,11 are the innermost part, fig. 11 being similar to fig. 10 but with artificial colours.

Figs. 5,6 represent the details of the minority of cuticles observed from another part of cuticle, with A2 granular layer of the cuticle proper in the outer part, fibrillar (arrows) B1 layer in the middle and lower parts of the cuticular layer. Fig. 6 is similar to fig. 5 but with artificial colors.

Plate IX. Transmission electron microscopy, guard cell cuticles details.

Figs. 1-4 represent the details of the majority of cuticles observed, with only fibrillar (arrows) B1 layer of the cuticular layer. For fig. 2, number 4 represents the photo number of enlarged detail in photo 4.

Fig. 5 represents the details of the minority of cuticles observed, with A2 granular layer of the cuticle proper in the outer part, fibrillar B1 layer in the middle part and B2 granular layer of the cuticle proper in the innermost part, with artificial colors. Some very parallel lines may appear in some places, actually due to an artefact of the diamond knife and different from the B1 fibrils.

Figure 1. EDS statistics

Note- The Mann-Whitney test is used for evaluating the significant differences (or not) between chlorine Cl in the resin and the layers of upper and lower epidermal cell cuticles (A), then the differences between Sulfur S/ Calcium Ca ratios for these two remaining elements (B.).

Figure 2. Factorial component analysis with the six types of cuticles.

Figure 3. Factorial component analysis with layers thickness values and percentages.

Note- The membrane cuticle thickness CM can be made with CP (cuticle proper = A2) and Cl (cuticular layer = B1 (and B2), depending on each of the 6 types of cuticles.

Figure 4. Summary of Student's t-tests, ratios of the significant differences between thickness and percentage values of the layers of all types of cuticles.

Note- It is calculated, with the Student's t-test, with the ratio of the number of significant differences /total number of combinations between the layers for each type of cuticle, on a scale of 10 %. For instance, for upper OEC and CM, there are 4 significant differences with GC, simp and comp-pp, L-OEC) / 5 possibilities (one is unsignificant difference: SC with p value of 0.76), making a ratio of 0.8 (see Appendices D-E). 0.0 (white color) means 0 % of significant differences, 1 (1.0, dark green) means 100 % of significant differences. White blanks with no ratio correspond to an absence of layers in these types of cuticles. The ratios with values of layers (a) are followed by the ratios with thickness % of layers (b). The membrane cuticle thickness CM can be made with CP (cuticle proper = A2 layer) and Cl (cuticular layer = B1layer (and B2 layer), depending on each of the 6 types of cuticles Six types of cuticles are evaluated: for upper and lower ordinary epidermal cells OEC, compound and simple papillae, subsidiary and guard cells of the stomatal apparatus.

Figure 5. Percentages of independency between the layers of all six types of cuticles, based on thickness values of layers.

Note- It is a 3D summary representing the six types of cuticles, where the percentages correspond directly to the ratiosX100 of significantly different thickness values between all layers of appendix D, from 40% (lower independency between the thickness values

of the same layers of all types of cuticles = stronger common thickness values between them) to 100% (total independency = no common thickness values between them). In order to simplify the figure, as original percentages values contain decimas, for each type of cuticles the percentages are summarized on a scale of 10, while the means are indicated in their real values. The membrane cuticle thickness CM can be made with CP (cuticle proper = A2) and Cl (cuticular layer = B1 (and B2)), depending on each of the 6 types of cuticles.

Figure 6. Percentages of independency between the layers of all six types of cuticles, based on thickness percentages of layers.

Note- It is a 3D summary representing the six types of cuticles, where the percentages correspond directly to the ratios X100 of significantly different thickness percentages of all types of cuticles of appendix E, from 0% (no independency between the thickness % of the same layers of all types of cuticles = strongest common thickness % between them) to 100% (total independency = no common values between them). In order to simplify the figure, for each type of cuticles the percentages are indicated on a scale of 10, while the means are indicated in their real values. The membrane cuticle thickness CM can be made with CP (cuticle proper = A2) and Cl (cuticular layer = B1 (and B2), depending on each of the 6 types of cuticles.

Figure 7. Three-dimensional reconstruction of lower and upper cuticles of *Ptilophyllum eminelidarum.*

Note- It is constructed with all SEM and TEM details, for each of the six types of cuticles, percentages of each layer and the total cuticular membrane thickness are provided. OC= Outer chamber; IC= Inner chamber.

Figure 8. Dichotomous key and Hierarchical component analysis for the six types of cuticles.

Note- This dichotomous key enables to distinguish, from the top to the bottom of the key, each of the six types of cuticles, using the order and summarized thickness values or percentages of variables obtained by factorial component analysis (see Fig. 3). At the bottom of the figure is represented the Hierarchical component analysis of the six types of cuticles. The percentage of independency, evaluated from Student's t-test, is added for the three groups of ordinary epidermal cell, stomatal apparatus and papillae cuticles. The membrane cuticle thickness CM can be made with CP (cuticle proper = A2) and Cl (cuticular layer = B1 (and B2), depending on each of the 6 types of cuticles.

Appendix A. EDS original values.

Appendix B. Some FCA values.

Appendix C. video of FCA cuticles.

Appendix D. Student's t-test with thickness values of types of cuticles and their layers.

Appendix E. Student's t-test with thickness % of types of cuticles and their layers.

Appendix F. video of FCA variables.

Appendix G. Mann-Whitney EDS tests.

Declaration of interests

The authors declare that they have no known competing financial interests or personal relationships that could have appeared to influence the work reported in this paper.

Table 1. Statistical values, based on 30 measurements of the thicknesses for the cell cuticles.

Please note. Min-max = minimum and maximum values of thickness observed % = percentage of each detailed part of the cuticle; st-d = standard deviation. The cuticular membrane CM is made up with cuticle proper CP (= A = A2 layer) and cuticular layer CL (= B = B1 + B2 layers). All measurements are in nanometers.

	upper cuticle of ordinary epidermal cell				lower cuticle of ordinary epidermal cell			
	mean	min- max	%	st-d	mean	min- max	%	st-d
CM	1954.38	712.54-2732.81	100	824.75	1[illegible]3.49	765.88-2472.44	100	627.02
CP (A)	287.80	25.51- 759.52	14.72	225.88	203.89	96.93-376.234	14.42	91.36
A2	287.80	25.51-759.52	14.72	225.88	203.89	96.93-376.234	14.42	91.36
CL(B)	1666.58	669.76-2495.26-	85.28	681.22	1209.60	584.40-2165.95	85.58	546.14
B1	1345.90	626.31-2284.18	68.87	598.85	869.76	147.06-1717.13	61.53	506.36

B2	320.68	23.02- 797.89	16.41	239.64	339.84	22.48-1176.01	24.05	367.70

	simple papilla of lower cuticle				compound papilla of lower cuticle			
	mean	**min-max**	**%**	**st-d**	**mean**	**min-max**	**%**	**st-d**
CM	1228.99	1152.03-1399.12	100	54.31	534.15	406.12-649.56	100	103.22
CP (A)	110.07	72.56-158.24	8.96	22.46	106.06	71.31- 143.35	19.86	15.05
A2	110.07	72.56-158.24	8.96	22.46	106.06	71.31- 143.35	19.86	15.05
CL(B)	1118.92	1032.59-1310.35	91.04	58.16	428.09	301.59-545.07	80.14	100.12
B1	1118.92	1032.59-1310.35	91.04	58.16	428.09	301.59-545.07	80.14	100.12

	stomatal apparatus of lower cuticle							
	subsidiary cell cuticle				guard cell cuticle			
	mean	**min-max**	**%**	**st-d**	**mean**	**min-max**	**%**	**st-d**
CM	2105.54	110.44-9861.87	100	2572.75	333.66	90.09-1193.69	100	280.48
CL (B)	2105.54	110.44-9861.87	100	2572.75	333.66	90.09-1193.69	100	280.48

B1	210 5.54	110.44-9861.87	100	2572.75	333.66	90.09-1193.69	100	280.48

Highlights

- New data for *Ptilophyllum eminelidarum* Bennettitales, Lower Cretaceous of Patagonia
- 6 types of cuticles defined with TEM, with detailed 9 variables of layers
- Cuticles' and layers' hierarchy, with multidimensional analyses and Student's t-tests
- Dichotomous key allowing a rapid identification of each type of cuticle
- Sulfur/Calcium ratio through EDS, homogeneous for all layers

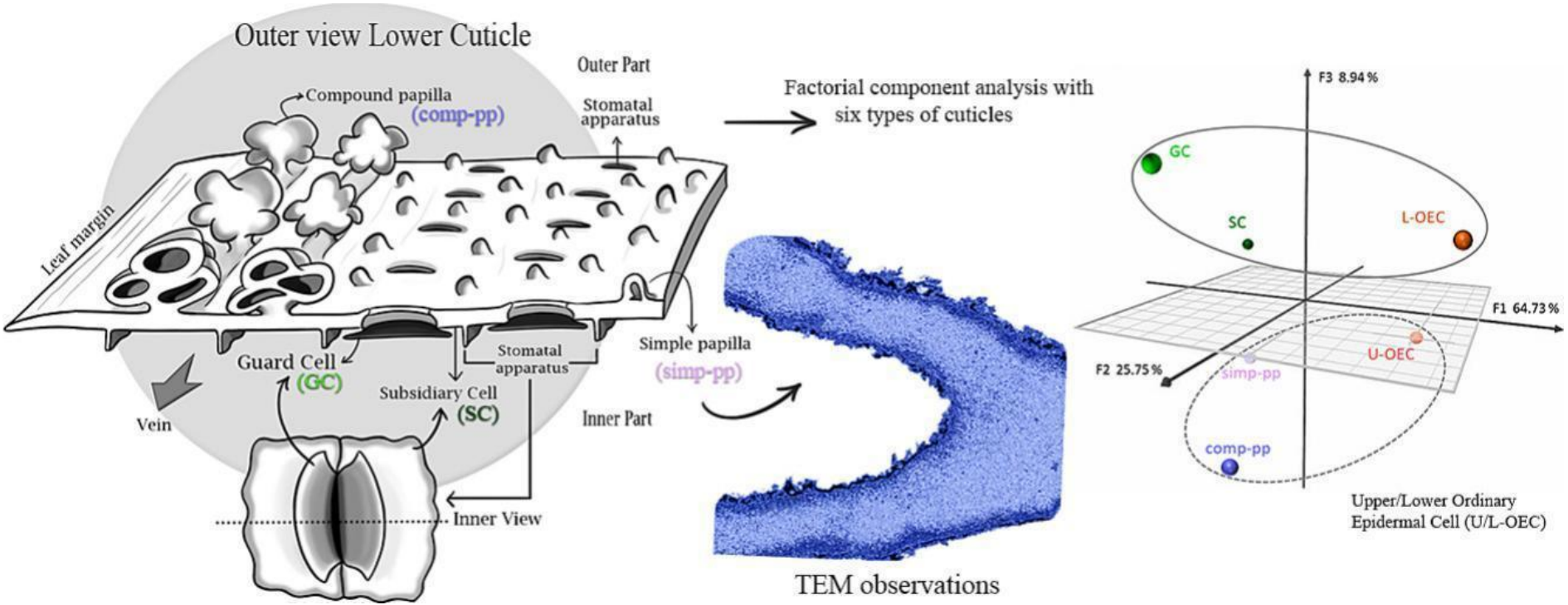

Graphics Abstract

A. Mean and confidence interval plus p value (CI)

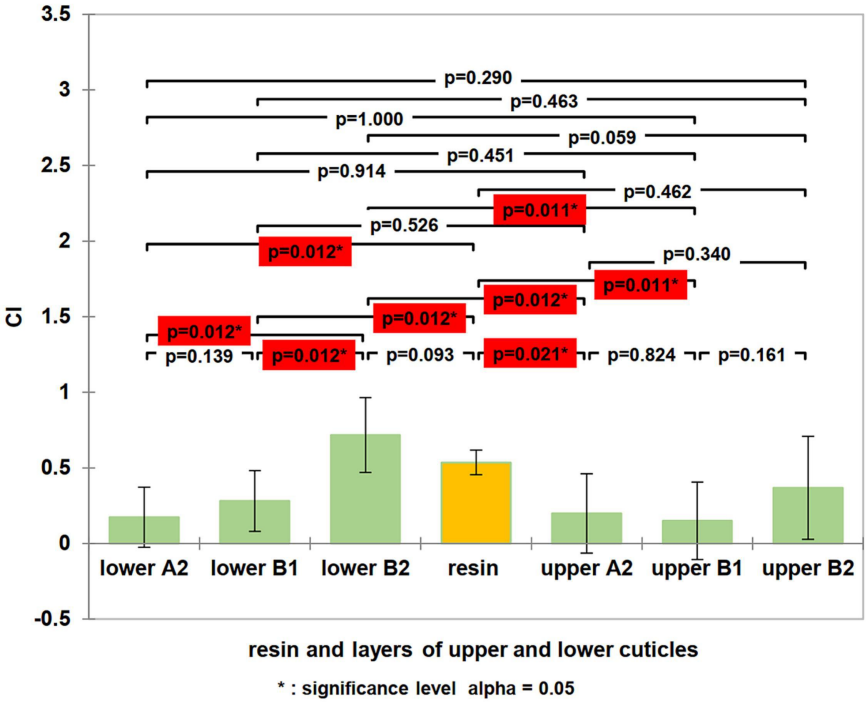

* : significance level alpha = 0.05

B. Mean and confidence interval plus p value (ratio S/Ca)

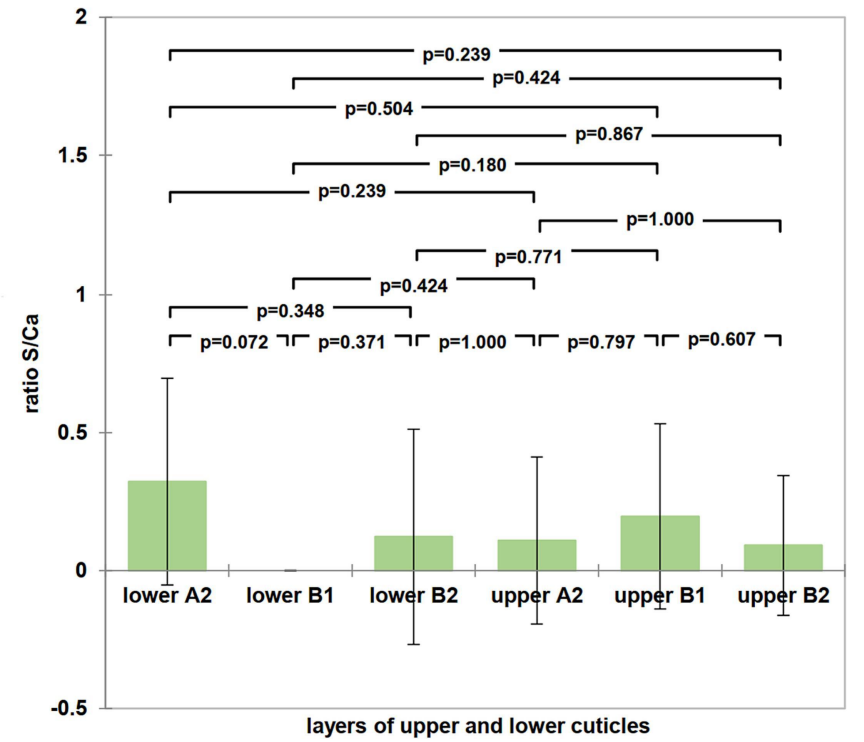

Figure 1

cumulative contribution
on axes F1. F2. F3

SC subsidiary cell cuticle	0.48
GC guard cell cuticle	0.44
L-OEC lower ordinary epidermal cell cuticle	0.44
U-OEC upper ordinary epidermal cell cuticle	0.32
comp-pp compound papilla cuticle	0.27
simp-pp simple papilla cuticle	0.20

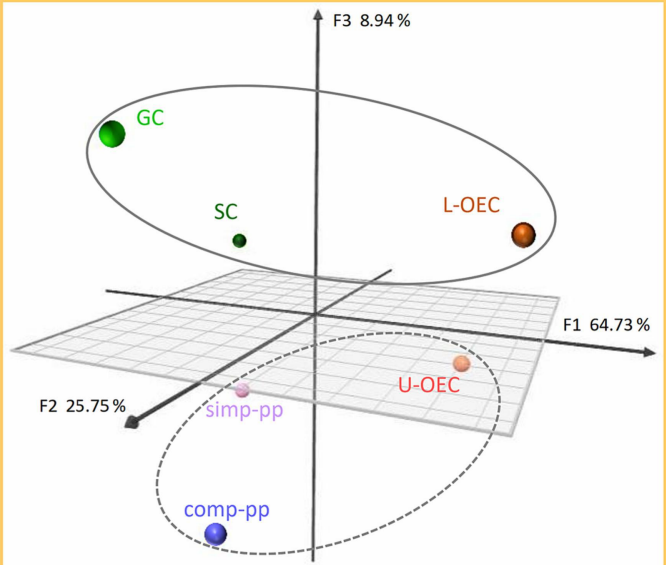

99.42 % of contribution of the three axes

Figure 2

cumulative contribution
on axes F1. F2. F3

B2 mean	0.549
A2 (CP)mean	0.416
B1%	0.326
CL %	0.283
B1 mean	0.264
B2%	0.145
A2%	0.139
CL mean	0.099
CM mean	0.075

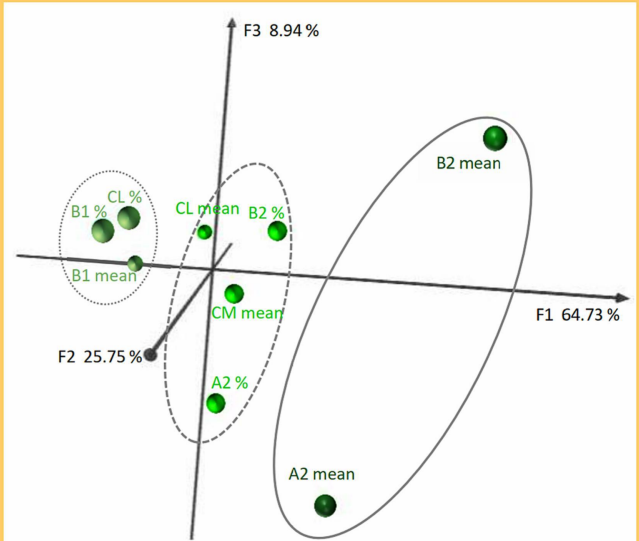

99.42 % of contribution of the three axes

Figure 3

a. ratios of the significant differences between values of layers and types of cuticles

	upper OEC	lower OEC	simple papilla	compound papilla	subsidiary cell	guard cell	total
cuticular membrane CM	0.8	0.6	0.6	1.0	0.4	1.0	0.7
cuticle proper CP = A2	0.8	0.8	0.8	0.8			0.8
cuticular layer B = B1 + B2	0.8	0.6	0.8	0.8	0.6	0.8	0.7
B1	0.8	1.0	1.0	0.8	0.8	0.8	0.9
B2	0.8	0.8					0.8
total	0.8	0.8	0.8	0.9	0.6	0.9	

b. ratios of the significant differences between proportions (%) of layers and types of cuticles

	upper OEC	lower OEC	simple papilla	compound papilla	subsidiary cell	guard cell	total
cuticle proper CP = A2	0.7	0.7	1.0	1.0			0.8
cuticular layer B = B1 + B2	0.8	0.8	1.0	1.0	0.8	0.8	0.9
B1	0.8	0.8	1.0	1.0	0.8	0.8	0.9
B2	0.0	0.0					0.0
total	0.7	0.7	1.0	1.0	0.8	0.8	

Figure 4

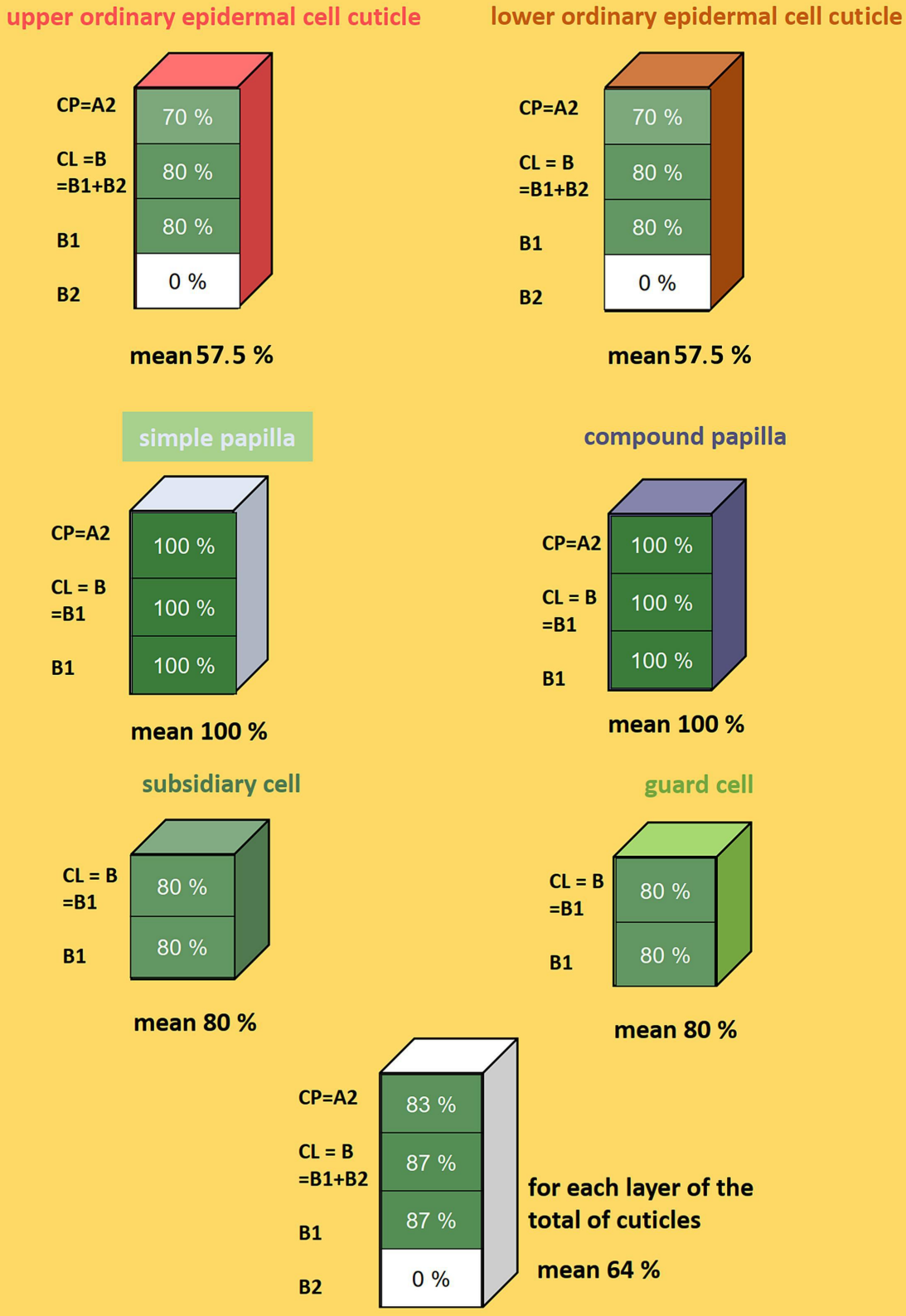
upper ordinary epidermal cell cuticle
CP=A2
CL =B
=B1+B2
B1
B2
70 %
80 %
80 %
0 %
mean 57.5 %
lower ordinary epidermal cell cuticle
CP=A2
CL = B
=B1+B2
B1
B2
70 %
80 %
80 %
0 %
mean 57.5 %
simple papilla
CP=A2
CL = B
=B1
B1
100 %
100 %
100 %
mean 100 %
compound papilla
CP=A2
CL = B
=B1
B1
100 %
100 %
100 %
mean 100 %
subsidiary cell
CL = B
=B1
B1
80 %
80 %
mean 80 %
guard cell
CL = B
=B1
B1
80 %
80 %
mean 80 %
CP=A2
CL = B
=B1+B2
B1
B2
83 %
87 %
87 %
0 %
for each layer of the
total of cuticles
mean 64 %

Figure 5

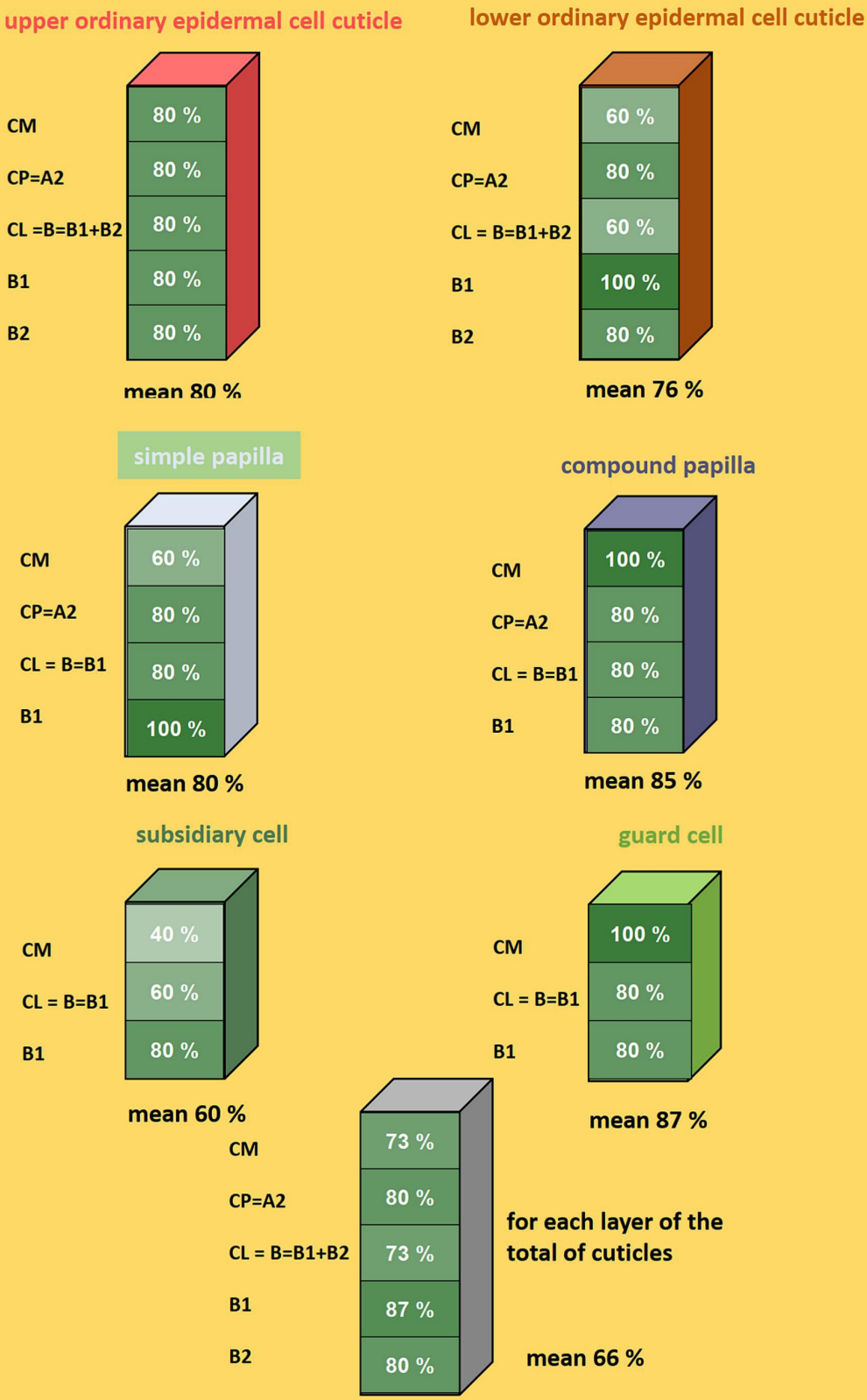
upper ordinary epidermal cell cuticle
CM
CP=A2
CL =B=B1+B2
B1
B2
80 %
80 %
80 %
80 %
80 %
mean 80 %
lower ordinary epidermal cell cuticle
CM
CP=A2
CL = B=B1+B2
B1
B2
60 %
80 %
60 %
100 %
80 %
mean 76 %
simple papilla
CM
CP=A2
CL = B=B1
B1
60 %
80 %
80 %
100 %
mean 80 %
compound papilla
CM
CP=A2
CL = B=B1
B1
100 %
80 %
80 %
80 %
mean 85 %
subsidiary cell
CM
CL = B=B1
B1
40 %
60 %
80 %
mean 60 %
guard cell
CM
CL = B=B1
B1
100 %
80 %
80 %
mean 87 %
CM
CP=A2
CL = B=B1+B2
B1
B2
73 %
80 %
73 %
87 %
80 %
for each layer of the
total of cuticles
mean 66 %

Figure 6

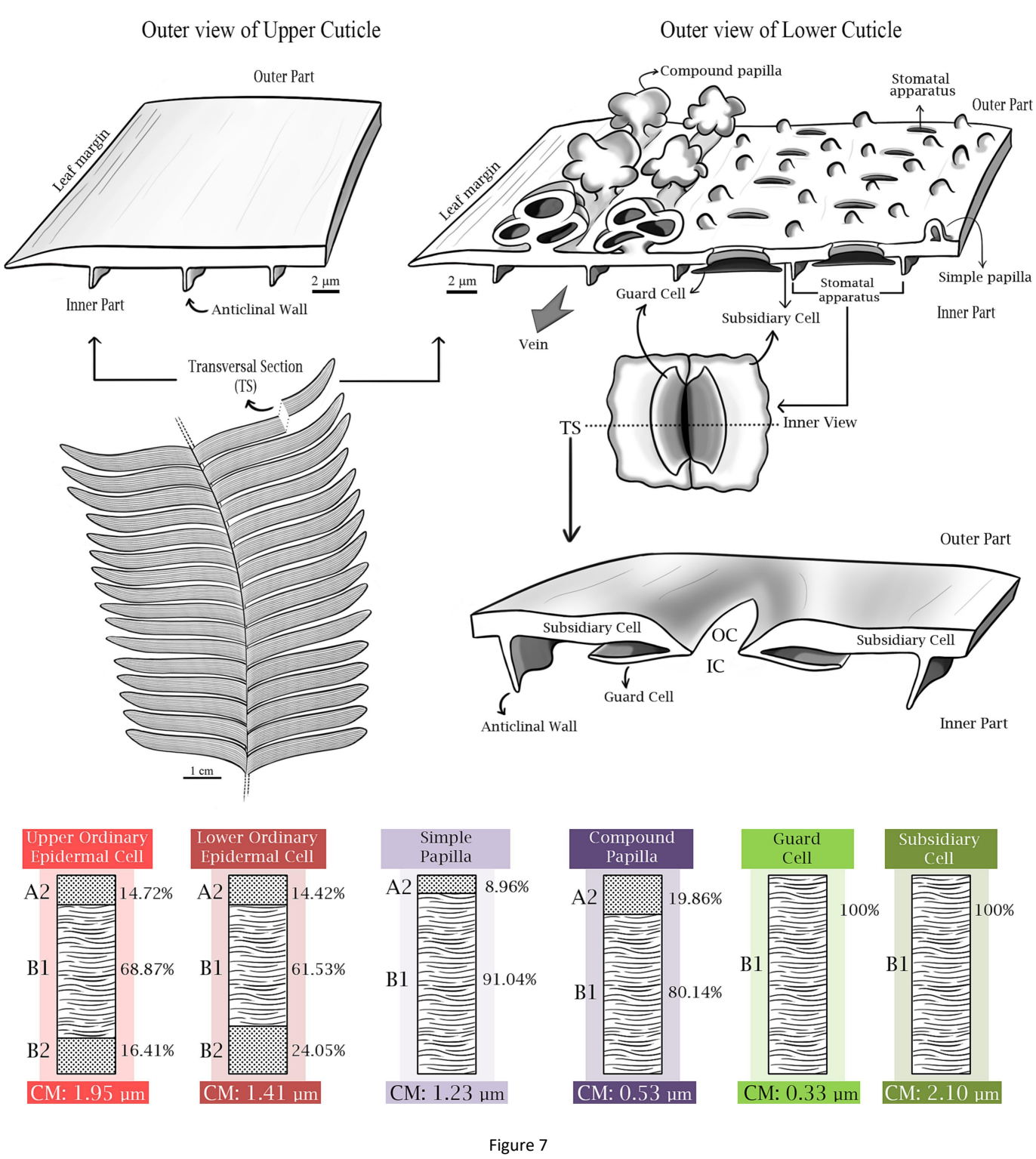
Outer view of Upper Cuticle
Outer Part
Leaf margin
2 µm
Inner Part
Anticlinal Wall
Transversal Section
(TS)
1 cm
Outer view of Lower Cuticle
Compound papilla
Stomatal
apparatus
Outer Part
Leaf margin
2 µm
Guard Cell
Stomatal
apparatus
Simple papilla
Inner Part
Subsidiary Cell
Vein
TS
Inner View
Outer Part
Subsidiary Cell
OC
IC
Subsidiary Cell
Guard Cell
Anticlinal Wall
Inner Part
Upper Ordinary Epidermal Cell
A2
14.72%
B1
68.87%
B2
16.41%
CM: 1.95 µm
Lower Ordinary Epidermal Cell
A2
14.42%
B1
61.53%
B2
24.05%
CM: 1.41 µm
Simple Papilla
A2
8.96%
B1
91.04%
CM: 1.23 µm
Compound Papilla
A2
19.86%
B1
80.14%
CM: 0.53 µm
Guard Cell
B1
100%
CM: 0.33 µm
Subsidiary Cell
B1
100%
CM: 2.10 µm

Figure 7

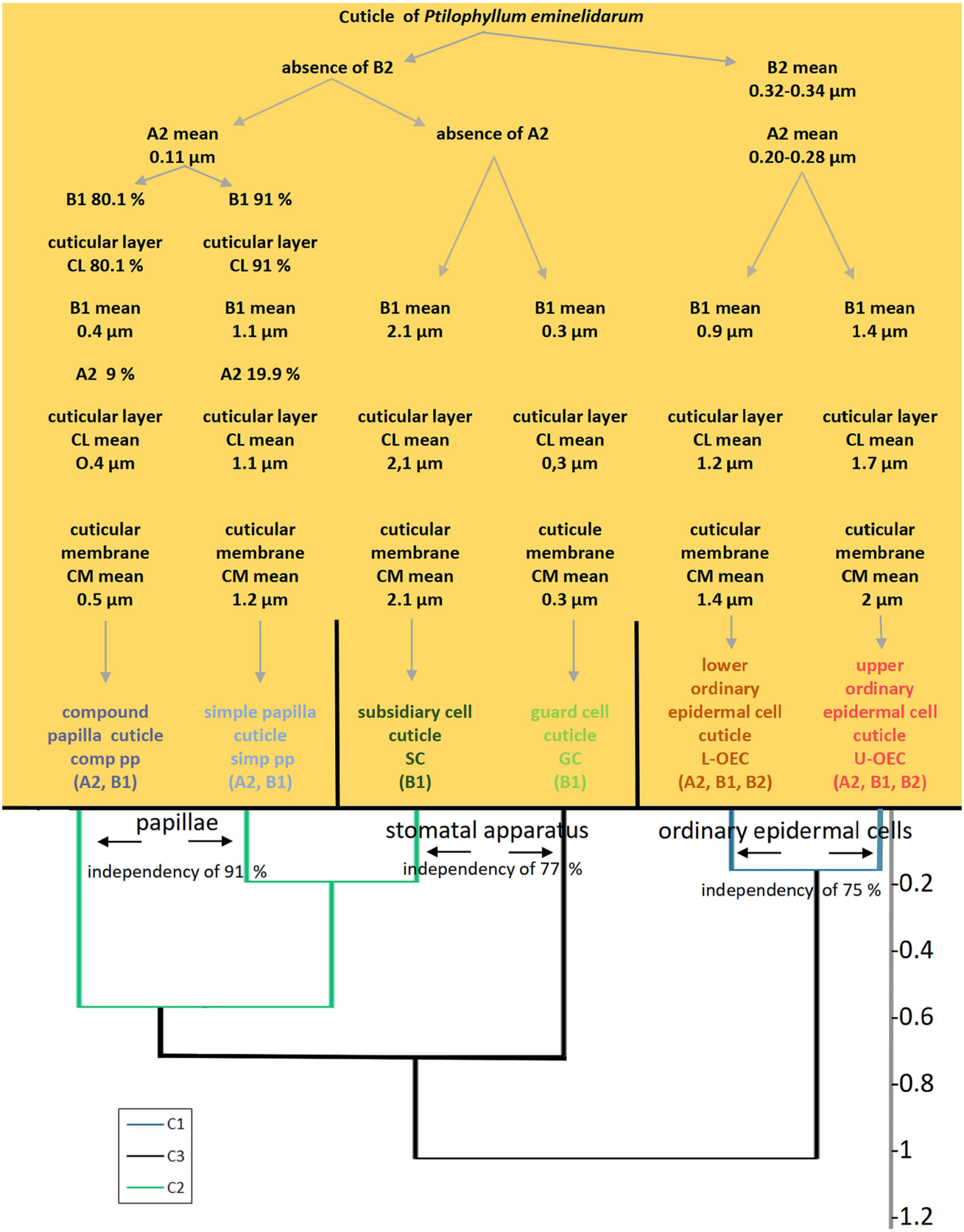
Cuticle of Ptilophyllum eminelidarum
absence of B2
B2 mean
0.32-0.34 µm
A2 mean
0.11 µm
absence of A2
A2 mean
0.20-0.28 µm
B1 80.1 %
B1 91 %
cuticular layer
CL 80.1 %
cuticular layer
CL 91 %
B1 mean
0.4 µm
B1 mean
1.1 µm
B1 mean
2.1 µm
B1 mean
0.3 µm
B1 mean
0.9 µm
B1 mean
1.4 µm
A2 9 %
A2 19.9 %
cuticular layer
CL mean
O.4 µm
cuticular layer
CL mean
1.1 µm
cuticular layer
CL mean
2,1 µm
cuticular layer
CL mean
0,3 µm
cuticular layer
CL mean
1.2 µm
cuticular layer
CL mean
1.7 µm
cuticular
membrane
CM mean
0.5 µm
cuticular
membrane
CM mean
1.2 µm
cuticular
membrane
CM mean
2.1 µm
cuticule
membrane
CM mean
0.3 µm
cuticular
membrane
CM mean
1.4 µm
cuticular
membrane
CM mean
2 µm
compound
papilla cuticle
comp pp
(A2, B1)
simple papilla
cuticle
simp pp
(A2, B1)
subsidiary cell
cuticle
SC
(B1)
guard cell
cuticle
GC
(B1)
lower
ordinary
epidermal cell
cuticle
L-OEC
(A2, B1, B2)
upper
ordinary
epidermal cell
cuticle
U-OEC
(A2, B1, B2)
papillae
independency of 91 %
stomatal apparatus
independency of 77 %
ordinary epidermal cells
independency of 75 %
0.2
0.4
0.6
0.8
1
1.2
C1
C3
C2

Figure 8